ABSTRACT

Title of Document:	Estimation of the Time of Concentration with High-Resolution GIS Data: Limitations of Existing Methods and Analysis of New Methods.
	Sandra B. Pavlovic, Master of Science, 2007
Directed By:	Dr. Glenn E. Moglen, Department of Civil and Environmental Engineering

Differences in the calculation of the time of concentration using the velocity method result from different degrees of discretization along the longest flowpath in the watershed. We examined an idealized system for which an analytical solution could be derived. Next, we studied a dataset compiled from watersheds across the State of Maryland, for which the observed time of concentration was known. In both cases we show that the time of concentration estimate increases with the degree of discretization.

Two different models were developed that show good predictive agreement with the observed time of concentration. One method uses, gradually varied flow concepts to allow velocity to vary more realistically along the discretized flowpath. The other method uses a regression approach to guide the merging of GIS pixel-based flowpath elements into larger segments. Strengths and limitations of both methods are discussed in the context of future application in Maryland and elsewhere.

Estimation of the Time of Concentration with High-Resolution GIS Data: Limitations of Existing Methods and Analysis of New Methods.

By

Sandra B. Pavlovic

Thesis submitted to the Faculty of the Graduate School of the
University of Maryland, College Park, in partial fulfillment
of the requirements for the degree of
Master of Science
2007

Advisory Committee:
Professor Glenn E. Moglen, Advisor
Professor Richard H. McCuen
Professor Kaye Brubaker

In memory of my father

Bozidar L. Pavlovic

Acknowledgements

I would like to show sincere gratitude to several people who influenced me both personally and professionally during the course of my studies. First, I am grateful to my advisor, Dr. Glenn E. Moglen, who continuously encouraged and supported me throughout this research. In addition to his dedicated advising, valuable ideas and discussions, he also made the research extremely enjoyable and fun for me. Further, I would like to thank Dr. Richard H. McCuen for his immense help during this research, for his insightful suggestions and for expanding my knowledge of hydrology. I would also like to thank Dr. Kaye L. Brubaker, Dr. Charles W. Schwartz, and Dr. Deborah J. Goodings.

I would like to acknowledge my office mates, Anuba, Alfonso, Dori, David, Jeff, Karthik, Melih and Sarah, for creating a collegial atmosphere and a great work environment.

Last, but certainly not the least, I thank my family (my mom Jelisaveta and my sister Tijana) and friends for their help and support, and for being the source of my endless enjoyment. Primarily, I am grateful for knowing they are always with me, in all of my endeavors. Thanks!

Table of Contents

List of Tables

List of Figures

Terminology

t_c - Time of concentration.

t_p -"pixel-based" time of concentration is derived with velocity method on each pixel along the longest path within GIS.

t_s - "single-segment" time of concentration is derived with velocity method on one merged segment for each flow type (overland, swale, pixel) along the longest path within the GIS.

t_{obs} -"observed" time of concentration is derived by Thomas et al. (2002) from observed runoff and rainfall measured data collected by the Dillow et al. (1998).

t_r - "reference" time of concentration model. Time of concentration derived based on a regression equation developed by the Thomas et al. (1998) based on the t_{obs} and watershed characteristics collected by Dillow et al. (1998).

$GVF_{c,s}$ -gradually varied flow in channel with single-segment approach used for overland and swale portion of the flow path.

$GVF_{c,p}$ - gradually varied flow in channel with pixel-based approach used for overland and swale portion of the flow path.

$GVF_{o,s}$ -gradually varied flow including the overbank part of channel flow with pixel-based approach used for overland and swale portion of the flow path.

$GVF_{o,p}$ - gradually varied flow including the overbank part of channel flow with single-segment approach used for overland and swale portion of the flow path.

t_v - "time-area" time of concentration based on a average portion of drainage area that contributes runoff at outlet for the observed time of concentration.

t_{uh} -"time-area" time of concentration based on the routed time-area diagram through a series of single liner reservoir (*SLR*).

$t_{p,scs}$ -is time of concentration developed by dividing the t_p by three based on SCS dimensionless unit hydrograph theory.

t_m - time of concentration based on the merging the number of segments along the longest flow path in time at the watershed based on the regression equation developed this study.

Chapter 1: Introduction

1.1 Introduction

The time of concentration, t_c, is defined as the "time it takes for runoff to travel from the hydraulically most distant part of the storm area to the watershed outlet or other point of reference downstream." (SCS,1972). This is the time at which, theoretically, the entire watershed is contributing to flow at the outlet. Some factors that influence the time of concentration are the watershed area, slope, and channel roughness. This time dimension is important because it attributes a representative time scale to the watershed that characterizes the speed at which the watershed responds to rainfall events.

Many commonly used hydrologic models require information about the time of concentration [e.g. HEC-HMS (USACE, 2001); TR-20 (SCS, 1986)] and numerous methods have been developed over the years to estimate the t_c (e.g. Kirpich, 1940; Izzard, 1946; Morgali and Linsley, 1965; and SCS, 1972). These models and methods reflect the numerical tools and data availability of their times often, using single estimates of quantities that can vary widely within the watershed such as slope, roughness, and land use.

Today, we have the powerful tool of geographic information systems (GIS) and a wealth of data in the form of digital topography, land use, and other information. Using a first-principles approach, the time of concentration can be derived by sub-dividing the longest (in time) flow path into small segments and then simply summing across all segments,

$$t_c = \sum_{i=1}^{n} \frac{\Delta L_i}{v_i} \qquad (1)$$

where ΔL_i is the length and v_i is the velocity for the i^{th} flow segment. The SCS velocity method (SCS, 1986) essentially uses equation 1 except that the SCS method distinguishes between three types of flow: sheet flow, swale flow, and open channel flow, each with its own equation defining travel time or velocity.

It has been observed that the SCS velocity method for estimating time of concentration calculated with high resolution GIS data gives unrealistically large values for the time of concentration (Pavlovic and Moglen, in press). Therefore, this study investigates the effects on time of concentration calculations as a function of level of discretization of the longest flow path and quantifies the difference between time of concentration estimates calculated using traditional methods with a coarsely discretized flow path compared to computational methods that take full advantage of the high-resolution of GIS data. The goal of this study is to develop an algorithm within the GIS to accurately match the observed time of concentration. This accuracy will be tested using an existing dataset in the state of Maryland.

1.2 Time of Concentration and Discharge

The time of concentration parameter is an important input in runoff-rainfall modeling. Rainfall-Runoff models like TR-55 (SCS, 1986), TR-20 (SCS, 1986) and HEC-HMS (USACE, 2001) are used to estimate the peak discharge which is used for design purposes for storm-water management systems, and bridge/culverts openings. Accurate estimates of the time of concentration are important. If time of concentration is over-estimated, the result is an under-estimated peak discharge. Likewise, an under-estimated time of concentration results in an over-estimated peak discharge. Pavlovic and Moglen (in press) show that coupling high-resolution GIS data with traditional methods for estimating the time of

concentration can produce estimates that are three to four times greater then observed time of concentration. In such a situation, the resulting rainfall-runoff model estimates peak discharge will likely be substantially smaller then the observed discharge.

There is a need to assess existing t_c methods within a GIS environment. This study addresses this need by evaluating existing methods for calculating the time of concentration and developing more appropriate time of concentration methods that can be applied within a GIS environment.

1.3 Research Goal and Objectives

The goal of this study is to develop a GIS-based approach that will accurately predict observed time of concentration for an existing dataset in the state of Maryland.

In order to achieve this goal, the following objectives are identified:

1. Investigate the effect of the level of discretization of the longest flow path on computed time of concentration.
2. Understand the factors that influence the velocity method computed on a small increment to produce a large time of concentration for watersheds.
3. Develop a method that produces accurate time of concentration estimates using the velocity method and high resolution data.
4. Adapt method for direct application within a GIS environment.

Chapter 2: Literature Review

2.1 Background

Many hydrologic models require a watershed characteristic that describes the timing of runoff. A number of time parameters have been developed that are used as the input in these hydrologic models. Historically, two distinct categories of travel times have emerged: time of concentration and lag time.

TR-55 (SCS, 1986) analysis recommends the velocity method for calculating the time of concentration. This velocity method distinguishes between three types of flow regimes: sheet, swale and channel flow. Sheet flow occurs in the upper-most portion of the flow path where runoff pathways are not well-defined. Within a maximum length of 91.44 m (300 feet), the sheet flow travel time is computed by the kinematic wave equation,

$$t_{sheet} = \frac{0.007(Ln)^{0.8}}{P_2^{0.5} S_x^{0.4}} \tag{2}$$

where L is the length of the overland flow in feet, n is the Manning roughness coefficient, S_x is the land slope in ft/ft, and P_2 is the 2-year, 24-hour rainfall in inches.

When the sheet flow starts to concentrate into the shallow channels, the swale portion of the flow begins. The average velocity of this portion of a flow is the function of slope and type of the channel (unpaved or paved). The velocity equation for a swale reach is,

$$v_i = kS_i^{0.5} \tag{3}$$

where k is a coefficient for type of the channel and S_i is the slope of the i^{th} reach.

Channel flow is assumed to begin where digitized "blue lines" from the USGS (2006) are indicated by National Hydrograph Dataset (NHD). The channel travel time equation is calculated by using Manning's equation for velocity,

$$v_i = \frac{1}{n} R_i^{2/3} S_i^{1/2} \quad (4)$$

where the R_i is the hydraulic radius in meters and S_i is the channel slope. The velocity method assumes bankfull flow, thus the bankfull flow hydraulic radius is used in equation 4. In order to quantify the relationship between drainage area and bankfull channel dimensions (depth and width), many states publish hydraulic geometry equations such as the U.S Fish and Wildlife equations in Maryland (McCandless and Everett, 2002; McCandless, 2003a, 2003b).

Time of travel for the swale and channel portions of the flow can then be calculated using equation 1 as the sum of the set of incremental travel times based on spatially varied measures of incremental flow path lengths and the associated velocities. The overall t_c for the watershed is the sum of the travel times from the separate flow regimes,

$$t_c = t_{sheet} + \sum t_{swale} + \sum t_{channel} \quad (5)$$

Lag travel time:

Lag travel time, t_{lag}, is defined as "the time from the center of mass of excessive rainfall to the peak rate of runoff" (SCS, 1972). There are different empirical equations developed for estimating the t_{lag}, the most common being the one developed by the NRCS (SCS, 1972),

$$t_{lag} = \frac{l^{0.8}\left(\frac{1000}{CN} - 9\right)^{0.7}}{1900 Y^{0.5}} \quad (6)$$

where t_{lag} is in hours, l is hydraulic length of the watershed in feet, CN is hydrologic soil cover and Y average watershed land slope in percent. The lag time mostly simulates concentrated flow (McCuen, 2005). The NRCS recommends that the lag equation be used

for watersheds of 8.1 km^2 (2000 acres) or less. However, McCuen et al. (1984) have shown that accurate estimates of t_c for up to 16.2 km^2 (4000 acres) can be made using the lag equation.

Although lag time and time of concentration both characterize the time scale of watershed response, they are not the same quantity. The relationship between the two is given by (SCS, 1972),

$$t_{lag} = 0.6t_c \tag{7}$$

The lag equation is adequate for non-urban homogeneous watersheds since it was developed using largely agricultural watershed data. This equation is easy to use since the watershed is represented with one equation, generalizing the runoff behavior for the entire basin.

2.2 Observed Time of Concentration

The time of concentration for a watershed can be derived from the observed rainfall hyetograph and runoff hydrograph. Since the time of concentration is defined as the "time required for a particle of water to flow hydraulically from the most distant point in the watershed to the outlet or design point" then the time from the end of the rainfall excess to first inflection point at the recession curve of the direct runoff hydrograph can be used to calculate time of concentration for each watershed (McCuen, 2005). The end of the rainfall excess is the point at which the last rainfall drop that falls on a watershed is contributing to surface runoff and the first inflection point at the recession curve of the hydrograph is the point where the surface runoff ends.

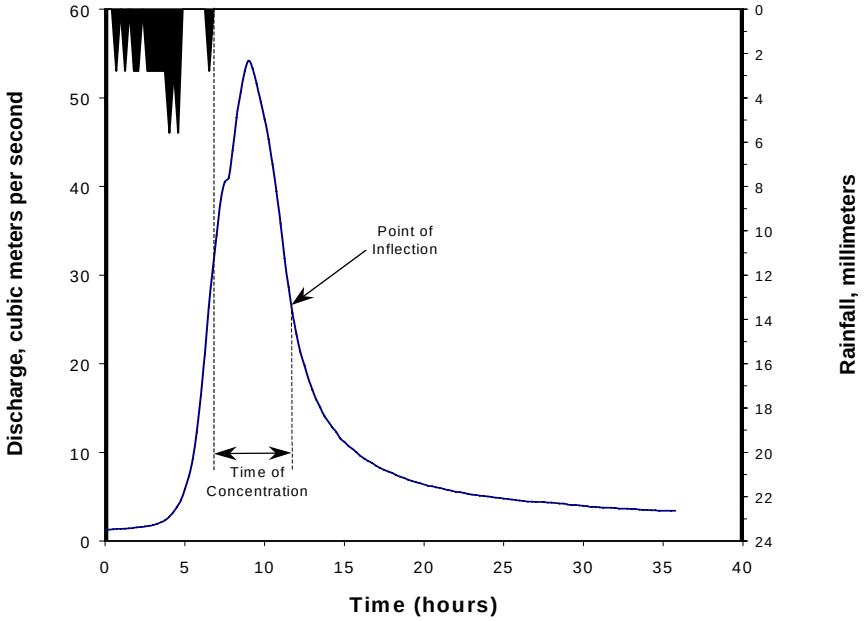

Figure 2-1: Observed time of concentration (Thomas et al. 2002).

Thomas et al. (2002) derived time of concentration based on this definition for 78 gaging stations in the state of Maryland which were previously collected as part of a flood hydrograph study for the Maryland State Highway Administration by Dillow in 1998 (Thomas et al., 2002). The observed time of concentration value derived by Thomas et al. (2002) was calculated based on three rainfall events, on average, for each watershed where the inflection point on the direct runoff hydrograph was easily detectable. These times of concentration are used within this study as the observed time of concentration, t_{obs}, for the study watersheds since they were derived based on the watersheds measured rainfall-runoff events. Time of concentration that was calculated with velocity methods and methods developed within this study are evaluated based on observed values of time of concentration.

2. 3 Reference Time of Concentration for State of Maryland by Thomas et al. (2002)

Historically, many equations developed for predicting the time of concentration or lag time are based on the empirical formulas for watersheds. These equations relate various watersheds characteristics like slope, drainage area, length, land use, etc. with a watershed time parameter like time of concentration or lag time. Kirpich (1940), the Federal Aviation Agency equation (1970), the SCS lag formula (1972), and the Eagleson lag model (1962) are only a few of the empirical equations that are frequently used to predict the timing of runoff for the watersheds.

Thomas et al. (2002) developed a regression-based equation for predicting the time of concentration parameter for the state of Maryland. They correlated the time of concentration to watershed characteristics like forest cover, impervious area, channel slope, channel length, and storage that were found to be the most significant among other watershed parameters evaluated with a step-wise regression method. The criterion variable, time of concentration, was based on the observed time of concentration, described in the preceding section. The regression equation they developed was based on a log-log transformation yielding the multinomial power correlation with observed time of concentration. Thomas et al. (2002) observed that the state of Maryland has three distinct physiographic regions: the Appalachian Plateau, Coastal Plain and Piedmont physiographic regions. A regression equation was developed for the Piedmont region and adjustment factors were included for the Appalachian Plateau and Coastal Plain regions. The equation developed by Thomas et al. (2002) is:

$$t_c = 0.133 CL^{0.475} SL^{-0.187} \left(101 - FOR\right)^{-0.144} \left(101 - IA\right)^{0.861} \left(ST + 1\right)^{0.154} \left(10^{0.194\,AP}\right)\left(10^{3.66\,CP}\right) \quad (8)$$

where t_c is time of concentration in hours, *CL* is channel length in miles, *SL* is channel slope in feet per mile, *FOR* is forest cover in percent, *IA* is impervious area in percent, *ST* is

storage (lakes and ponds) in percent. If the watershed is located in Appalachian Plateau, *AP* equals one, otherwise zero. Likewise, if the watershed is located in Coastal Plain, *CP* equals one, otherwise zero.

Regression equations are often used in engineering practice; however, they should be applied only to watersheds with similar characteristics to the watersheds characteristics that used to develop the regression equation. The time of concentration, developed by Thomas et al. (2002), hereafter will be referred as the reference time of concentration, t_r, and will be used as a reference model for predicting t_c for the new models developed in this study.

Chapter 3: Velocity Methods for Calculating Time of Concentration within GIS: Problems and Advantages

3.1 Experiment with an Idealized System

We begin by considering an idealized watershed in which the flow path controlling the time of concentration has uniform characteristics throughout. In this example, only slope will be varied although, in general, other channel characteristics such as roughness or geometry also vary spatially. We consider two systems where the elevation along the longest flow path is defined by equations 9 and 10,

$$y_1 = x \tag{9}$$

$$y_2 = x^2 \tag{10}$$

where y is elevation x is position along the flow path, measured from upstream to downstream. For simplicity, we will examine a unit length of the flow path from $x = 0$ to $x = 1$. Slope along the longest flow path is simply,

$$S_1 = \frac{dy_1}{dx} = 1 \tag{11}$$

$$S_2 = \frac{dy_2}{dx} = 2x \tag{12}$$

Assuming channel flow and either a Manning's or Chézy velocity relationship,

$$v \sim \sqrt{S} \tag{13}$$

where v is the velocity. Incremental travel time, dt_c is just the incremental distance divided by the velocity,

$$dt_{c,1} = c\frac{dx}{\sqrt{S}} = c \cdot dx \tag{14}$$

$$dt_{c,2} = c\frac{dx}{\sqrt{S}} = c\frac{dx}{\sqrt{2x}} \tag{15}$$

where c is a constant that is dependent on roughness and channel geometry. The total travel time is just the integral of equations 14 and 15,

$$t_{c,1} = c\int_0^1 dx = c\left[x\right]_0^1 = c \tag{16}$$

$$t_{c,2} = \frac{c}{\sqrt{2}}\int_0^1 \frac{dx}{\sqrt{x}} = c\left[\sqrt{2x}\right]_0^1 = c\sqrt{2}\cdot\left(\sqrt{1}-\sqrt{0}\right) = c\sqrt{2} \tag{17}$$

For simplicity, we assume that c=1, then the travel time over this unit length segment is just 1 for profile 1 and $\sqrt{2}$ for profile 2. For contrast, Table 2-1 shows the travel time if the channel is treated as having one, two, three, or an infinite number of segments over the distance from $x = 0$ to $x = 1$.

Table 2-1: Time of concentration in two idealized systems as a function of number of segments.

Num. of Segments							t_c		t_c	
	x	$y_1=x$	$y_2=x^2$	$S_1=\frac{\Delta y_1}{\Delta x}$	$S_2=\frac{\Delta y_2}{\Delta x}$	Δx	$\frac{\Delta x}{\sqrt{S_1}}$	$\frac{\Delta x}{\sqrt{S_2}}$	$\sum\frac{\Delta x}{\sqrt{S_1}}$	$\sum\frac{\Delta x}{\sqrt{S_2}}$
1	0.0	0.0	0.0						1.0	1.0
				1.0	1.0	1.0	1.0	1.0		
	1.0	1.0	1.0							
2	0	0	0						1.0	1.115
				1.0	0.5	0.5	0.5	0.707		
	0.5	0.5	0.25							
				1.0	1.5	0.5	0.5	0.408		
	1.0	1.0	1.0							
3	0.0	0.0	0.0						1.0	1.147
				1.0	0.333	0.333	0.333	0.577		
	0.333	0.333	0.111							
				1.0	1.0	0.334	0.334	0.334		
	0.667	0.667	0.444							
				1.0	2.0	0.333	0.333	0.236		
	1.0	1.0	1.0							
∞	--	--	--	--	--	--	--	--	1.0	$\sqrt{2}$ =1.41

This table clearly conveys that as level of discretization increases, so does the estimate for the travel time.

3.2 Velocity Method Time of Concentration:" Pixel-based" and "Single-segment" Time of Concentration

Using a first-principles approach, the time of concentration can be derived by sub-dividing the longest (in time) flow path into small increments and simply summing the calculated time for each increment to derive the overall travel time. This could be modeled within a GIS environment by using digital elevation model (DEM) data to generate the longest flow path. By applying the velocity method equation for the time of concentration

for each pixel, one can calculate the overall time of concentration for a watershed. However, while time of concentration generated within the GIS grows larger with higher discretization as in the theoretical model, it may not achieve higher accuracy. A longer time of concentration is a typical finding with calculating the time of concentration at a high level of discretization (Pavlovic and Moglen, in press). This finding is more likely to occur in relatively flat topography and is more pronounced in larger watersheds (watersheds in excess of 13.0 km^2 (5.0 mi^2)).

In order to demonstrate this discretization issue, 73 watersheds throughout the state of Maryland were delineated within the GIS (Figure 3-1). Time of concentration was calculated using 30 meter resolution DEM data and the NRCS velocity method (1986) approach. The longest flow path in the watershed was determined for incremental lengths of the flow path (either 30 or $30\sqrt{2}$ meters). The sheet portion of the flow, with a maximum length of 30.5 meters (100 feet) was calculated by summing the incremental travel times along every pixel on this portion of the flow. The parameters for the sheet t_c equation (equation 2) use the 2-year, 24-hour precipitation depth as determined by the NOAA Atlas 14 dataset (Bonnin, et al., 2004), and slope for each pixel calculated as the difference in elevation between the upstream and downstream pixel divided by the incremental flow length. The channel portion of the flow was determined using the National Hydrography Dataset (USGS, 2006) streams to indicate the location (and onset) of channel flow. For channel pixels, incremental travel times were calculated using Manning's equation. So as not to engage issues of sensitivity of t_c to channel roughness, a default value of 0.05 for Manning's n was used for all channels. Bankfull channel geometry was assumed for each segment based on the hydraulic geometry relationships developed for Maryland by the U.S. Fish and Wildlife Service

(McCandless and Everett, 2002; McCandless, 2003a and 2003b). Cumulative travel time along the channel portion of the flow gave the travel time for the channel section. The swale portion of the flow was taken as any remaining flow length that was neither sheet nor channel. Equation 3 was used assuming an unpaved condition. This time of concentration will be hereafter be referred to as the "pixel-based approach" time of concentration.

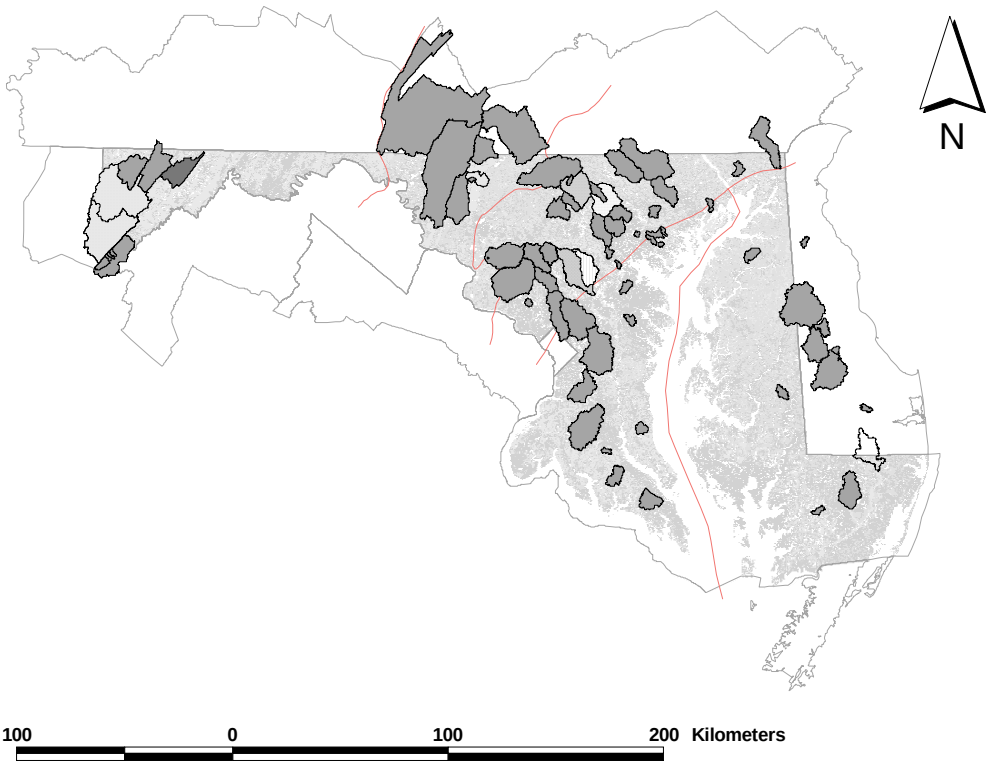

Figure 3-1: Spatial locations of delineated watersheds in Maryland dataset.

The "single-segment approach" treats the sections (overland, swale and channel) each as a single element, where the slope of the section is determined using the overall loss in elevation divided by the overall flow length. To compare with the pixel-based time of concentration, two different times of concentration approaches were derived for each watershed. The first approach includes the observed time of concentration, while the second

approach utilizes the single-segment time of concentration. While the number of pixels along the longest path for the pixel-based approach differs for each watershed, the single-segment approach has a constant number of increments.

Each delineated watershed thus had three estimates of the t_c. These values are shown in Figure 3-2 using the t_{obs} as the reference (horizontal axis) value.

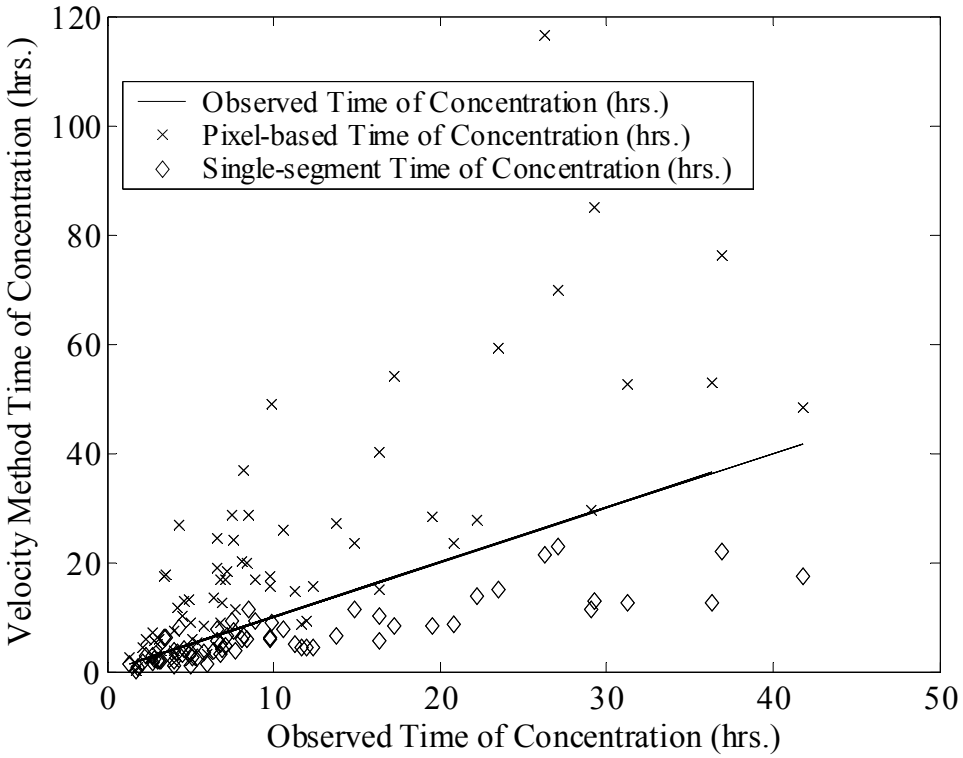

Figure 3-2: Time of concentration using different time of concentration approaches for the Maryland dataset.

Figure 3-2 shows that the single-segment time of concentration tends to agree more closely with the observed time estimate than does the pixel-based approach. As the size of the drainage area of the watershed increases, the discrepancy between the pixel-based approach and the observed t_c estimate tends to grow. Thus, Figure 3-2 does convey the general tendency for the pixel-based approach to over-predict t_c relative to the observed t_c

estimates. A systematic under estimation bias between the pixel-based and single-segment approaches is evident as the t_c increases with overall watershed size.

The importance of this observation is that velocity method applied to small flowpath increments (pixel-based approach) would tend to over-estimate time of concentration thus the peak discharge at the watershed outlet.

3.3 Velocity Method Calculation for Time of Concentration: Longitudinal Flow Discretization, Bankfull Flow Assumption and Sensitivity Analysis

Two major problems were identified with the velocity method approach for calculating the time of concentration within the GIS. The first problem concerns the small slopes generated when using the GIS. The velocity method was originally developed and used for calculating the time of concentration using much coarser flow path segments than those that can be generated by GIS. With the ability to generate the high resolution flow paths, as allowed by 30 and even 10 meter resolution DEM data, slopes determined by such small flow increments can yield very small (or even zero) values. Small slopes result in small velocity estimates and thus, high travel times. Moreover, the assumed uniform bankfull flow conditions on each pixel do not account for the potentially large variation in slope along the flow path that often leads to changing flow regimes from pixel to pixel. In reality, the flow is passing through riffle-pool sequences that correspond to both supercritical and subcritical flow conditions along the flow path. When the longest path is modeled using a longer section, the reality of riffle-pool sequences may be lost, but the overall normal depth for the length-averaged slope may lead to a more appropriate overall average flow velocity and thus produce a more accurate travel time estimate.

Manning's velocity equation is very sensitive to small slopes. The relative sensitivity of the input parameters in the Manning's velocity equation shows that the Manning's roughness coefficient and hydraulic radius have greater relative importance than the slope parameter, based on the exponent of the parameters in the equation. However, sensitivity of the output, in this case velocity, depends also on the magnitude of the input parameters (Manning's roughness, hydraulic radius, and channel slope). Thus, to show likely magnitudes of the channel velocities, the possible range of the channel slopes, and hydraulic radius based on hydraulic geometry equations (McCandless and Everett, 2002; McCandless, 2003a and 2003b) were evaluated. A Manning's roughness value of 0.05 was uniformly applied for consistency across the state of Maryland. Figure 3-3 shows the possible range of the calculated velocity for the given magnitudes of the hydraulic radius and localized channel slopes. For a constant value of the slope, the velocity relationship is more closely linear than the velocity relationship with a constant value of hydraulic radius. The small values of velocity which produce greater values of the travel time are more evident with the smaller values of slope than with smaller values of the hydraulic radius. This is expected since slopes have much smaller magnitudes than the hydraulic radius. Overall the average velocity for channel flow should be on the order of 1 to 2 ft/s. However, Figure 3-3 shows that many points (marked as *) are located well below this threshold value (2 ft/s). Some of the watersheds in the study dataset have more then 70% of the longest flow path sections with slopes less then 0.001 ft/ft which yields average velocity much below 2 ft/s plane. As a consequence, Manning's velocity calculated on each section over the longest path with very small values of localized slopes yields large (and possible too large) values of t_c.

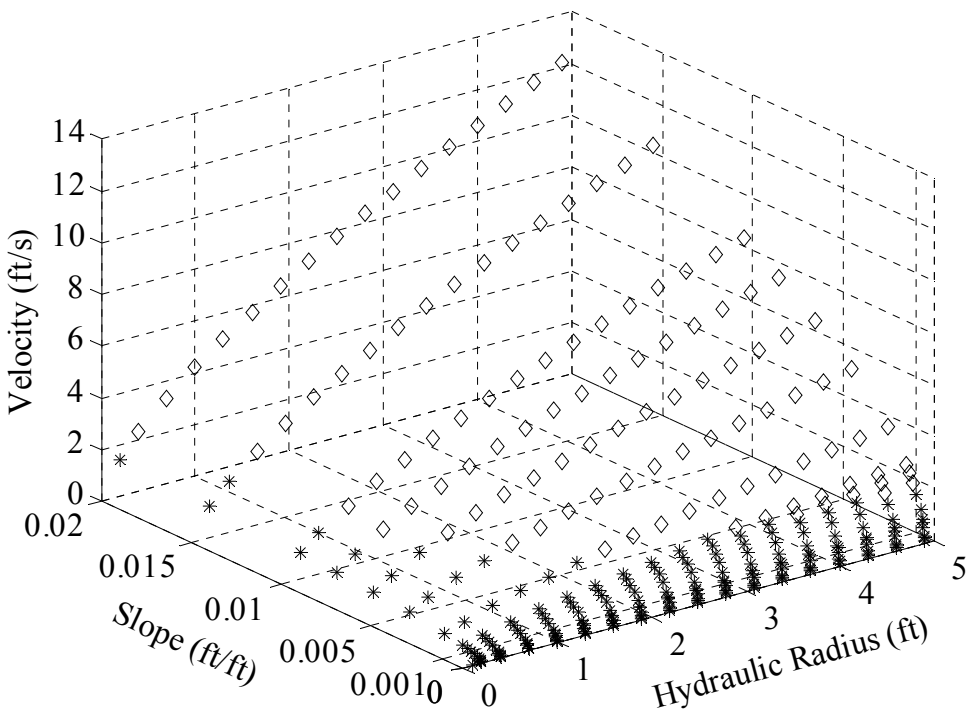

Figure 3-3: Calculated velocity as a function of the slope and hydraulic radius input values in the Manning's velocity equation.

The second problem with velocity method approach, when applied to channel flow, concerns the bankfull flow assumption. When bankfull geometry is defined by the regional curve depending only on a drainage area, then the bankfull flow assumption is not consistent with continuity. For instance, bankfull flow on a segment with a mild slope would imply a small discharge while bankfull flow on a steep slope segment would imply a large discharge. In either sequence, if these two segments are adjacent there is a discontinuity of discharge at their point of connection. Thus, by applying the assumed bankfull flow conditions for each segment regardless of the local slope, continuity of discharge is neglected and the realism of the velocity method for estimating time of concentration is lost.

For these reasons, increased discretization of the longest flow path may not produce more accurate estimates of the time of concentration. One reasonable solution to this discretization issue would be to merge individual segments into larger segments. In this way, the travel time calculation within the GIS interface would more closely resemble the traditional method of travel time calculation. Moreover, owing to the structure of DEM data and its tendency to produce small slope estimates for a pixel-based description of the longest flow path, larger segments generated by the judicious merging of individual pixels would tend to result in greater average slopes, greater velocities, and smaller, more realistic incremental travel times.

To demonstrate this effect, a watershed located in the Piedmont region with a drainage area of 23.3 km^2 (9.0 mi^2) was delineated. This is a USGS gaged watershed with station ID 01496200. An overall time of concentration of 8.27 hours was determined for the channel portion of the flow over the 268 individual channel pixels. When the whole channel length was treated as one segment, the time of concentration for the channel was reduced to 3.38 hours. The two estimates differ by a factor of 2.4. To examine the effect of channel discretization, the channel was sub-divided into a range of segment lengths, so that the total number of segments ranged from 1 to 268. The resulting time of concentration varies with the number of channel segments as shown in Figure 3-4.

For direct comparison to the observed time of concentration, Figure 3-4 shows the total t_c determined two different ways. The "Overall t_c (varying number of segments)" points (plotted with a "◊") show total t_c calculated treating the overland flow and swale flow portions of the t_c flow path as individual pixel segments. This represents the maximum t_c that can be calculated for these portions of the flow path. At the other extreme, the "Overall

t_c (Single-segment non-channel)" points (plotted with a "x") show the total t_c when overland flow and swale flow are determined from single-segments, representing the minimum t_c for these portions of the flow path. For this particular watershed, Figure 3-4 indicates that using approximately 35 channel segments produces an overall t_c that is close match to the observed time of concentration for this watershed.

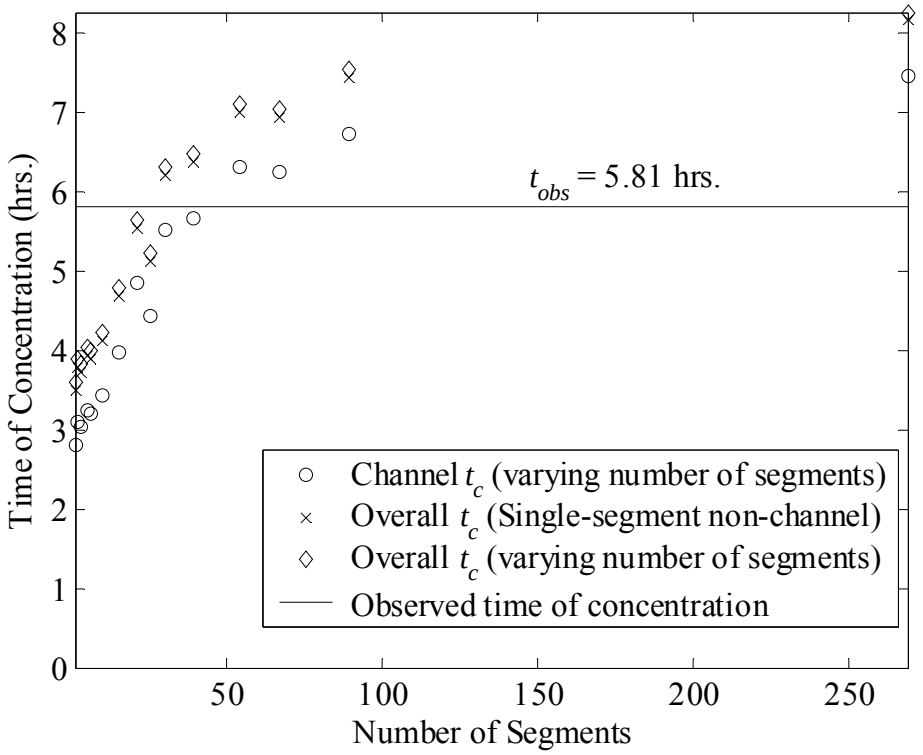

Figure 3-4: Velocity method t_c as a function of the number of channel segments used.

While this result may hold true for this particular watershed, it provides little insight into an overall approach for anticipating the range of t_c values that might be calculated depending on the number of segments used to characterize the longest flow path, nor does it provide a general method that could be applied to other watersheds. A general method will be developed in Section 4.3.

3.4 Maryland Time of Concentration Dataset from Thomas et al. (2002)

The dataset used in this study is based on a dataset previously assembled by Thomas et al. (2002). The Thomas dataset consist of 78 watersheds; however, only 73 of these watersheds were used in this study (Figure 3-1). Two watersheds, located in Delaware, were excluded since these watersheds do not drain into Maryland so the DEM was not readily available. However, six other watersheds from Delaware in the eastern Coastal Plain region that drain into Maryland were included in the study dataset. One watershed was excluded since it is a sub-watershed of an already included watershed and its drainage area comprises more then 50 percent of the drainage area of the included watershed. A watershed with drainage area consisting of the sum of four other study dataset watersheds was also excluded from the study dataset. Finally, one last watershed was omitted because the gage station drainage area reported by USGS differed from the GIS-based calculated drainage are by 24 percent, indicating a possible error in locating the watershed outlet or delineating the watershed. Appendix A lists the excluded watersheds and their gage station ID's.

Thomas et al. (2002) categorized watersheds into three distinct physiographic regions: Appalachian Plateau, Coastal Plain, and Piedmont. They defined the Blue Ridge sub-region as part of Piedmont Region based on Dillow's recommendations (Dillow, 1998). This study considers the Blue Ridge sub-region a part of the Appalachian Plateau region based on the Fish and Wildlife recommendations as shown in Figure 3-5 (McCandless and Everett, 2002; McCandless, 2003a and 2003b). In addition, the Thomas dataset watersheds were attributed to one of the regions based on the outlet location of the watershed. Since a watershed may have its outlet location in one region while some or most of the watershed drainage area is in another region; this study assigned watersheds into the regions based on

the location of the majority of the drainage area (more then 50 percent). If a watershed resides in more then one region, watershed characteristics (width, depth and bankfull discharge) were calculated based the area-weighted average of the corresponding Fish and Wildlife physiographic region equation coefficients.

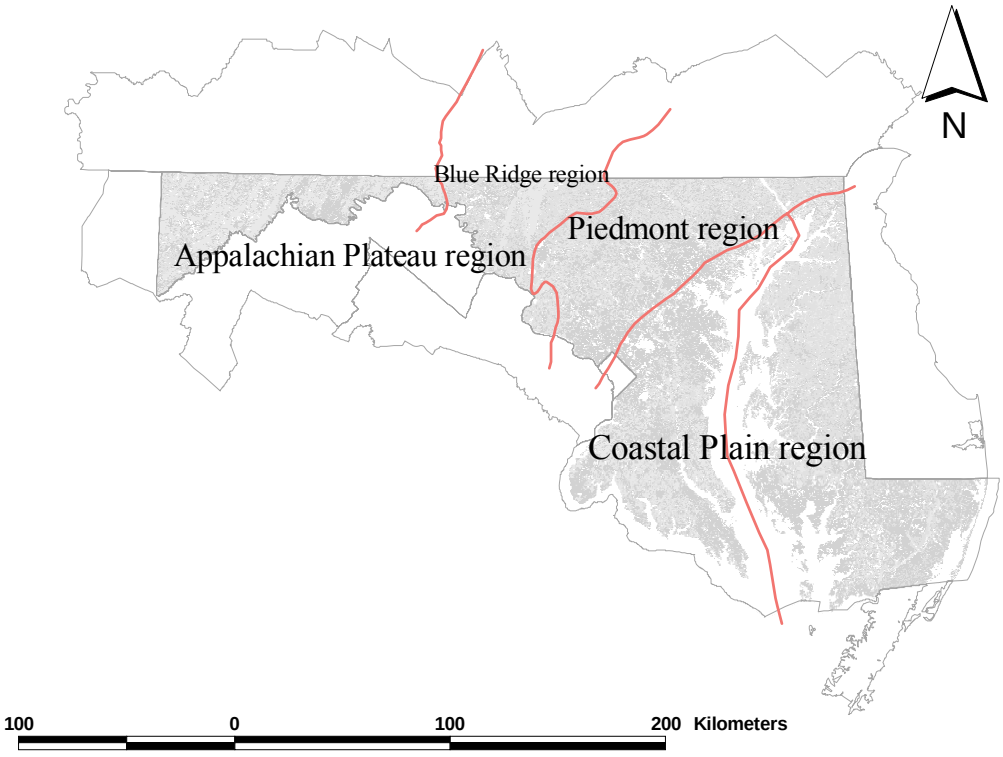

Figure 3-5: Physiographic regions within Maryland.

The velocity method single-segment and pixel-based time of concentration were calculated for all 73 watersheds as discussed in Chapter 3. Appendix B includes the gage stations ID numbers, observed travel time, single-segment and pixel-based t_c values for each delineated watershed. As previously shown, the observed travel time more closely matches the single-segment time of concentration than the pixel-based approach. However, the single-

segment time of concentration generally under-predicts the observed time of concentration values. The difference between the single-segment and pixel-based approaches varies with the watershed characteristics and the region where the watershed is located. This is expected since the Appalachian Plateau region is more steep and mountainous and thus the longitudinal profile in this region more closely resembles the single-segment profile. As will be examined more closely in Chapter 4 and 5, in the Coastal Plain, which has flatter topography than the other two regions, the pixel-based profile and resulting time of concentration more closely matches the observed time of concentration.

3.5 Quality of Predicting the Time of Concentration: Goodness-of-Fit Statistics

In order to measure prediction capacity of all models that are evaluated in this study, Goodness-of-Fit (GOF) statistics were calculated. Goodness-of-Fit statistics used in this study are based on the relative standard error of estimates (*Se/Sy*) and relative bias ($\bar{e}/\bar{y}$). The relative standard error of the estimate assesses the sample variation around the observed time of concentration and is calculated with the following equation:

$$Se/Sy = \frac{\sqrt{\frac{1}{n-2}\sum_{i=1}^{n}\left(t_{c,i}^{'} - t_{obs,i}\right)^2}}{\sqrt{\frac{1}{n-1}\sum_{i=1}^{n}\left(t_{obs,i} - \overline{t_{obs}}\right)^2}} \qquad (18)$$

where $t_c^{'}$ is the time of concentration based on the assessed model, $t_{obs,i}$ is the observed time of concentration values based on Thomas et al. (2002) dataset, and $\overline{t_{obs}}$ is the mean value of the t_{obs}. The relative standard error of the estimate is also sensitive to the number of watersheds in the dataset (n). Greater values of n allow for the better prediction of the model. However, even when the dataset has a small sample size, *Se/Sy* illustrates the prediction

capacity of the model. Small values of the relative standard error indicate a good prediction capacity of the model, while values greater then 1 indicate poor, if not irrational, model prediction.

Even though the relative standard error of the estimate shows the accuracy of the model, it does not capture whether there exists a systemic bias of the model. Relative bias ($\bar{e}/\bar{y}$) shows the degree by which the model over-predicts or under-predicts the observed time of concentration, on average. Positive values of the relative bias indicate that the model over-predicts the observed time of concentration. Negative values suggest under-prediction. Relative bias is calculated using the following equation:

$$\frac{\bar{e}}{\bar{y}} = \frac{\frac{\sum_{i=1}^{n}\left(t_{c,i}^{'} - t_{obs,i}\right)^2}{n}}{\frac{1}{n}\sum_{i=1}^{n} t_{obs,i}} \tag{19}$$

In this study, the coefficient of correlation does not accurately show the prediction capacity of the model, since, in some of the regions, the watersheds have a significantly larger observed times of concentration, compared to the remainder of the dataset, thus resulting in a greater value of the coefficient of correlation. Moreover, the coefficient of correlation can yield high values, even in cases where the model has a significant positive or negative bias, erroneously indicating a satisfactory model.

Chapter 4: Modeling and Data Analysis

4. 1 Gradually Varied Flow Analysis

4.1.1 Background

The pixel-based approach to estimate time of concentration assumes uniform flow at bankfull depth on each pixel segment, independent of the segment's upstream and downstream boundary conditions. Continuity of both discharge and flow depth is thus ignored. A more realistic assumption is to model the discharge moving though a series of a single pixel reaches, allowing for gradually varied (non-uniform) flow over each pixel.

Gradually varied flow is defined as a "steady flow whose depth varies gradually along the length of the channel" (Chow, 1959). Steady flow assumes that flow characteristics (depth, velocity, and channel-cross section) do not change over time but may change in space. Manning's velocity equation assumes that the normal depth is achieved on the flow sections when the channel slope is used instead of the water surface slope. This may hold true if the sections are long enough that the normal depth could be established along the section; however when variation of the slopes and channel cross-section with respect to distance is short, normal depth will generally not be established. Instead, flow will gradually accelerate or decelerate depending both on the channel characteristics and boundary conditions of the given flow section while changing from one flow condition to another. Gradually varied flow takes into account the changing watershed's characteristics along the channel and simulated changes of flow regimes between the sections. In this way, flow in one pixel can now influence conditions in neighboring pixels.

There are various techniques to calculate the water surface profile along the channel. The most common and accurate technique to calculate the water surface profile in natural channels is the standard-step method (Chow, 1959). The standard-step method employs the energy equation calculated from one section to another where energy losses are calculated with Manning's equation. The momentum equation is used for calculating the hydraulic jump and its location along the channel reach. This is an iterative technique, demanding non-trivial computational capabilities. This method allows the specification of one discharge at the upstream end of the channel reach and for the specification of the discharge at various locations along the channel. Figure 4-1 shows a watershed with a longest path divided into several sections. Specifying the discharge at each section, gradually varied flow becomes consistent with increasing discharge in the channel as more drainage area contributes to the channel while also satisfying the continuity of a discharge and depth between the flow sections on the longest path. These concepts are violated with the uniform, bankfull flow velocity method approach.

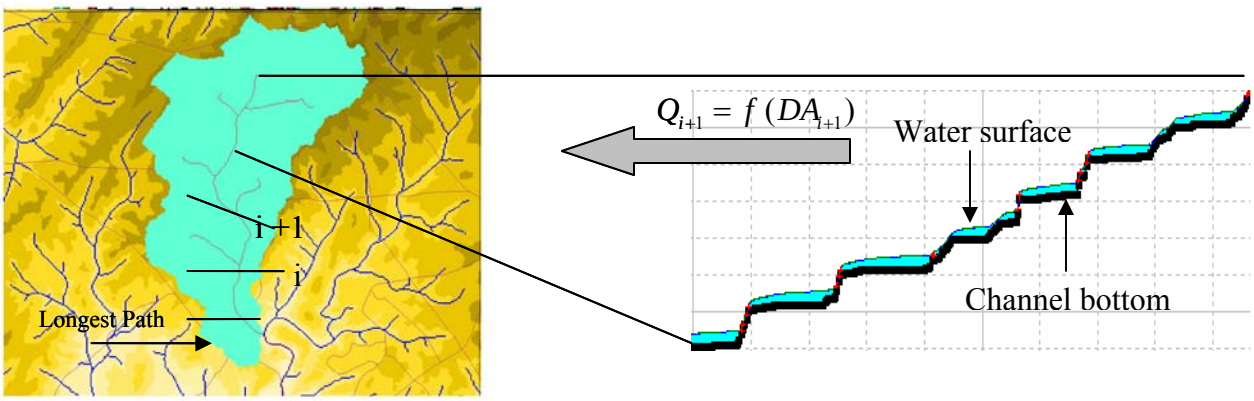

Figure 4-1: An illustration of gradually varied flow as modeled along short segments within the GIS.

If the longest flow path concept is to be maintained, the uniform, bankfull flow velocity method approach is not adequate for the longest flow path that is subdivided into small increments. Instead, gradually varied flow analysis should be applied since it accurately simulates the flow that, in reality, is passing through riffle-pool sequences that correspond to both supercritical and subcritical flow conditions along the flow path while maintaining both continuity of discharge and depth between individual flow segments.

4.1.2 Methodology: Gradually Varied Flow Analysis

The HEC-RAS and/ or HEC-2 program (USACE, 2001) is an appropriate tool for performing gradually varied flow calculations with the standard step method. The gradually varied flow time of concentration was calculated with the HEC-2 program for each watershed in the study dataset.

In order to run the HEC-2 program, an input file with channel characteristics (cross-section, length, elevation and discharge at each section) was derived from high-resolution GIS data. Channel sections were evaluated based on digitized "blue lines" from the USGS (2006) that are indicated by National Hydrograph Dataset (NHD) at a 1:100,000 mapping scale. The elevation and longest path length were derived from the DEM while width and depth of the stream were calculated based on the regional equations from the U.S. Fish and Wildlife Service for the middle pixel of the flow segment. (McCandless and Everett, 2002; McCandless, 2003a and 2003b). The bankfull discharge was also calculated based on the U.S. Fish and Wildlife Service regional equations ($Q_{bf} = c_1 A^{c_2}$) where drainage area at the middle pixel of the flow segment was attributed to the beginning of each flow segment. In this way, the discharge along the longest path changes as the drainage area increases along

the longest path (Figure 4-1). Therefore, the same information which is used in calculating the single-segment and pixel-based approach was used in the gradually varied flow analysis.

During the HEC-2 analysis it was observed that the gradually varied flow method is sensitive to the small slopes that were generated within the GIS. These small slopes led to small conveyance which tended to force flow out on the channel banks. Even though the channel geometry was derived with the U.S. Fish and Wildlife Service regional equations for the bankfull flow conditions, the gradually varied flow method calculated that a considerable portion of the flow is forced out of the channel. An overbank flow problem arose due to the regional equations and the methodology of relating the bankfull discharge with bankfull cross-section geometry. The regional regression equations relate stream slope, bankfull width and depth at the outlet point to the bankfull (approximately 1.5 year recurrence interval) discharge. Since the overbank flow observed with the HEC-2 analysis was localized where the small or flat slopes existed, we concluded that when these hydraulic geometry equations are applied along the longest path, the localized slopes have significant influence in determining the capacity of the channel cross section to contain the flow. Both the travel time of the channel portion of the flow and the overall travel time (that includes both channel and overbank flow) were evaluated. These travel times will be hereafter referred to as GVF_c and GVF_o travel time that stands for "gradually varied flow channel" and "gradually varied flow an overbank" travel times, respectively.

The travel time of the channel section that was calculated using gradually varied flow methods (GVF_c and GVF_o) within HEC-2 was summed with travel times for the non-channel portion of the flow that included both the overland and swale portion of the flow within the watershed. Such travel times were calculated using both single-segment and

pixel-based approaches. This gives four different variations of the gradually varied flow time of concentration:

Table 4-1: Gradually varied flow channel and non-channel flow variations.

Name	Channel Flow	Non-channel Flow
$GVF_{c,s}$	neglect overbank flow	Single-segment
$GVF_{c,p}$	neglect overbank flow	Pixel-based
$GVF_{o,s}$	include overbank flow	Single-segment
$GVF_{o,p}$	include overbank flow	Pixel-based

Appendix C contains an input file for the HEC-2 analysis developed within the GIS. The example of the input file is shown in Figure C-2.

4.1.3 HEC-RAS vs. HEC-2 Modeling

Water surface profile calculations using the standard step method can be calculated with both HEC-RAS and HEC-2 programs. HEC-RAS is a newer and more user-friendly version of the HEC-2 program. We had performed both HEC-RAS and HEC-2 analyses to compare the results and computational capabilities between these two programs. The same input files were used in the HEC-2 and the HEC-RAS programs, expecting the same results. The gradually varied flow analyses for the channel conveyed flow GVF_c were almost identical. However, gradually varied flow overbank GVF_o differed considerably. This difference is due to a different conveyance method techniques used by these two programs. Figure 4-2 below shows GVF_c and GVF_o travel time calculated with both HEC-2 and HEC-RAS programs for a set of study watersheds in the Piedmont Region.

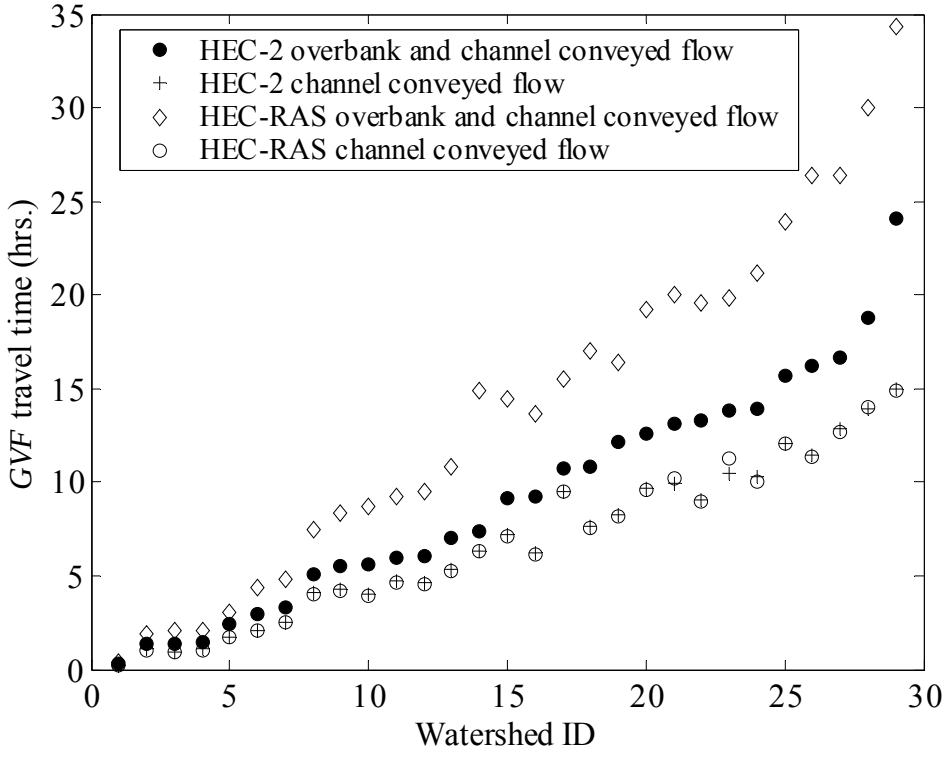

Figure 4-2: Difference in calculated travel times based on computational technique in the HEC-RAS and HEC-2 programs.

Since the overbank gradually varied flow analysis results differed depending on the model used, the author chose to focus on the channel portion of the flow, GVF_c in further analysis since it is more consistent across the two HEC programs. Nonetheless, Goodness-of-Fit (GOF) statistics were calculated for all four permutations of the gradually varied flow derived with the HEC-2 program which were less sensitive to small localized slopes along the longest path than HEC-RAS program.

4.1.4 Results and Discussion: Gradually Varied Flow Analysis

The times of concentration that were derived with the gradually flow method, $GVF_{c,s}$, $GVF_{c,p}$, $GVF_{o,s}$ and $GVF_{o,p}$ were evaluated based on two GOF statistics: relative

standard error (*Se/Sy*), and relative bias ($\bar{e}/\bar{y}$). Relative standard error of estimated is calculated with the following equation:

$$Se/Sy = \frac{\sqrt{\frac{1}{n-2}\bullet\left(t_{GVR} - t_{obs}\right)^2}}{\sqrt{\frac{1}{n-1}\sum_{i=1}^{n}\left(t_{obs,i} - \overline{t_{obs}}\right)^2}} \qquad (20)$$

where the observed time of concentration is the criterion variable and the time of concentration derived for each *GVF* method is the estimated prediction variable. This equation assumes that the correlation is linear.

Five of 27 Coastal Plain watersheds with all *GVF* methods performed poorly in predicting the observed time of concentration. The poor predictions of time of concentration for these watersheds were attributed to the long travel time for the swale portion of the flow even when calculated with a single-segment approach. The long travel time for the swale portion of the flow is caused by the flat topography for the non-channel portion of the longest flow path. Since Manning's equation (eq. 4) is used to calculate velocity, a small hydraulic radius (constant in eq. 3) and small slope generated irrationally small velocities and thus irrationally long travel times for the swale portion of the flow (Figure 3-3). These watersheds are omitted from further analysis; however, it is recommended that for watersheds with a travel time above seven hours, the single-segment swale portion of the flow be calculated based on the overall single-segment approach. The Figure 4-3 shows the omitted watersheds. The omission of the five watersheds reduces the size (*n*) of the dataset from 73 to 68 watersheds.

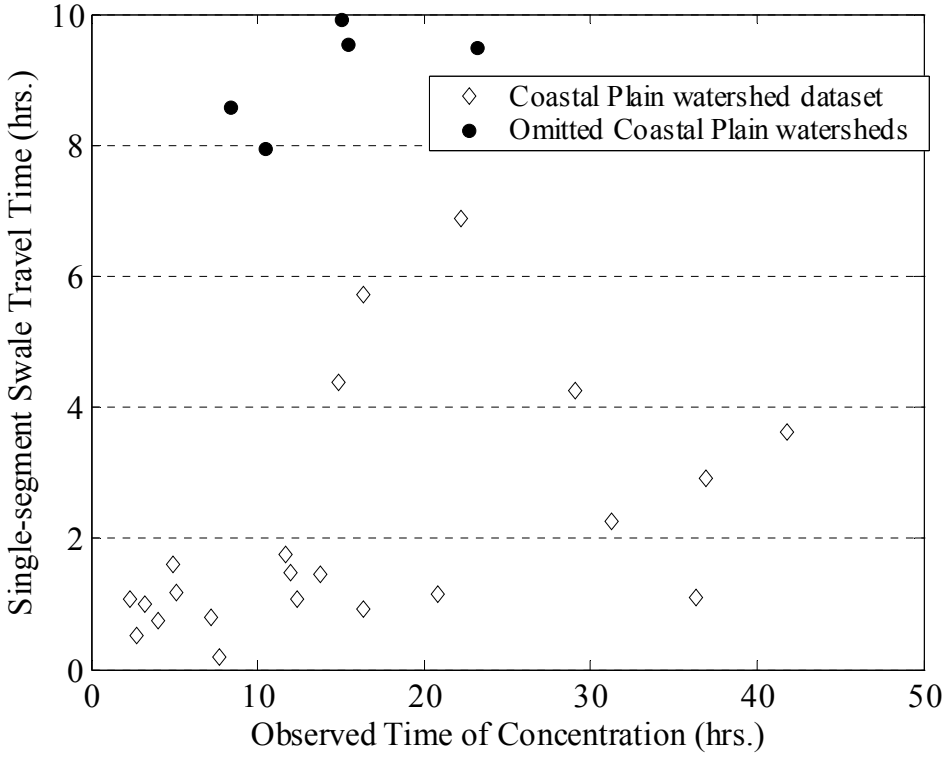

Figure 4-3: Single-segment swale travel time values in the Coastal Plain region. Omitted watersheds based on the seven hour single-swale travel time threshold are shown in black circles.

Table 4-2 shows the Goodness-of-Fit statistics (GOF) of the *GVF* analysis. Both the $GVF_{o,p}$ and $GVF_{o,s}$ perform poorer than the $GVF_{c,s}$ or $GVF_{c,p}$. This indicates that the channel only modeling is superior to the overbank modeling approach. Additionally, the channel only perspective has the advantage of being less sensitive to the detail of the calculation technique performed and/or program used. When $GVF_{c,s}$ and $GVF_{c,p}$ are compared based on their GOF statistics, $GVF_{c,p}$ shows better performance then $GVF_{c,s}$ since relative bias is smaller for the Coastal Plain region. The model performance in the Piedmont Region is poor with *GVF* analysis in general; however, this effect may be due to heavy

urbanization in this region as will be discussed in Chapter 5. Gradually varied flow simulates only the mechanics of the channel flow while observed time of concentration takes into account other watershed characteristics like impervious areas and forest cover which could speed up or delay the timing of runoff. The Piedmont Region has the greatest density of the impervious area in the state of Maryland since both the Washington D.C. and the Baltimore metropolitan areas are located in this physiographic region. GOF for the *GVF* approach needs to be compared to other methods to assess the best time of concentration prediction method.

Table 4-2: Goodness-of-Fit Statistics for *GVF* analysis.

Region	GOV Statistics	$GVF_{c,s}$	$GVF_{c,p}$	$GVF_{o,s}$	$GVF_{o,p}$
Appalachian Plateaus Region (*n*=17)	*Se/Sy*	0.51	0.51	0.97	1.01
	$\bar{e}/\bar{y}$	0.06	0.10	0.35	0.39
Coastal Plain Region (*n*=22)	*Se/Sy*	0.74	0.62	0.55	0.59
	$\bar{e}/\bar{y}$	-0.30	-0.18	-0.03	0.10
Piedmont Region (*n*=29)	*Se/Sy*	1.3	1.41	2.4	2.54
	$\bar{e}/\bar{y}$	0.33	0.44	0.76	0.87
State of Maryland (*n*=68)	*Se/Sy*	0.61	0.56	0.73	0.77
	$\bar{e}/\bar{y}$	-0.06	0.04	0.26	0.36

Overall, $GVF_{c,p}$ performs best across the watersheds analyzed in this study. The author selected this method to be the representative method for gradually varied flow analysis. In Chapter 5, the $GVF_{c,p}$ method will be compared to the other (existing and developed within this study) methods for predicting the time of concentration.

4.2 Time-area Unit Hydrograph Analysis

The velocity method calculates the time of concentration using the longest flow path in time concept. Within the GIS, the travel time for each pixel in the watershed is calculated

using the appropriate overland, swale and channel velocity equation. Each pixel, therefore, has an arrival time that contributes at the watershed outlet. By grouping the arrival times, the time-area diagram is developed. The flow path that produces the longest time is the pixel-based time of concentration, t_p, which represents the base of the time-area diagram. We have compared t_p to the observed time of concentration t_{obs}, which is defined as the time from the end of the rainfall excess to the first inflection point on the recession hydrograph curve (Figure 2-1). Even though both the pixel-based and the observed times of concentrations are based on time, not distance, they do not necessary reflect the same travel time since the time base is different than the time from rainfall excess to point of inflection.

The pixel-based time of concentration reflects only the mechanics of the watershed flow while the observed time of concentration is affected by other watershed characteristics like degree of urbanization, forest cover, and storage. The measured hydrograph that was used to calculate the observed time of concentration may be accelerated or delayed as a consequence of the land use which the pixel-based time of concentration velocity method does not capture. Thus, an alternative for computing a time of concentration within the GIS is presented in this section.

4.2.1 Introduction

A time-area diagram is a cumulative frequency distribution that quantifies the fraction of the watershed area that at some specific travel time contributes to surface runoff at the outlet (Figure 4-4a). The derivative of the time-area diagram is the time-area-concentration diagram (Figure 4-4b). In the case of deriving the time-area diagram within the GIS, each 30 meter pixel within the watershed is modeled separately. The travel time for each pixel is computed with the velocity method approach. Figure 4-4b shows the time-area-concentration

diagram derived within the GIS with number of pixels as the ordinate and travel time at which this fraction of the pixels contributes to flow at the outlet on the abscissa. The time base of the time-area-concentration diagram is the time at which the entire watershed contributes to surface runoff at the outlet point which equals the pixel-based time of concentration. The time-area-concentration diagram quantifies the unique watershed shape, slopes and drainage structure of each watershed. In this work, SCS methods were used to determine velocities for each pixel within the watershed.

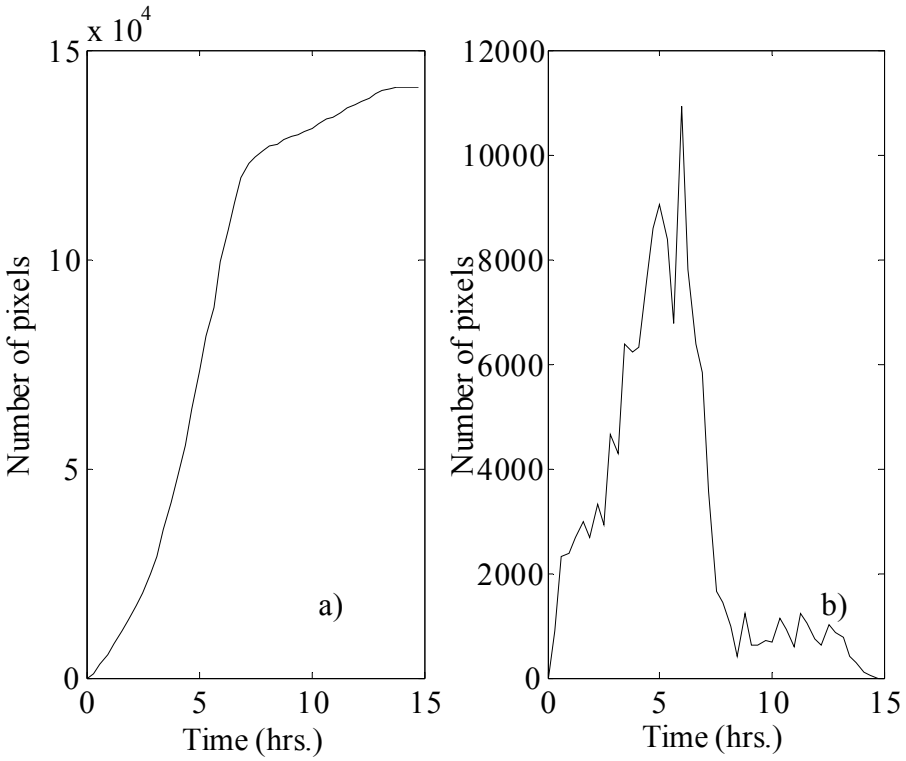

Figure 4-4: a) GIS-based time-area diagram developed with velocity method, b) GIS-based time-area-concentration diagram developed with velocity method.

A time-area-concentration diagram represents a conceptual hydrograph in which a burst of rainfall with unit volume occurs instantaneously. Thus, the time-area-concentration diagram is an instantaneous unit hydrograph (IUH). The instantaneous unit hydrograph

simulates surface runoff based only on the translation of water from one location to the next, ignoring watershed storage effects. A time-area diagram requires routing to reflect the effect of storage.

4.2.2 Time-area Methods Development

Three different time-area-based methods for estimating the time of concentration were studied. These methods employ the theoretical assumption of the SCS unit hydrograph approach, an empirical method based on the integral of the time-area-concentration diagram and converting the IUH to UH analysis, as will be explained in this section.

The rainfall-runoff model TR-20 (SCS, 1984) uses a dimensionless unit hydrograph to simulate a storm hydrograph for an ungaged watershed. The dimensionless unit hydrograph assumes that the time of concentration is the time from the end of rainfall excess to the first inflection point on the recession hydrograph curve. Since the pixel-based time of concentration is the base of the time-area-concentration diagram, a theoretical relationship between the dimensionless SCS unit hydrograph time of concentration and a dimensionless SCS unit hydrograph time base was developed. This relationship was then used to derive a time of concentration for the time-area-concentration diagram that is more consistent with the observed time of concentration.

Similarly, the second method uses the Thomas et al. (2002) dataset to determine the average fraction of area under the time-area-concentration diagram that corresponds to the observed time of concentration. The average fraction was then used to derive the time of concentration for each physiographic region in state of Maryland.

The third method is the most sophisticated. This method converts the instantaneous unit time-area diagram into a unit hydrograph by routing the time-area diagram through a

series of linear reservoirs. This method, therefore, included the watershed storage characteristics.

4.2.2.1 SCS-theory based Time-Area Method

The SCS TR-20 model uses a dimensionless unit hydrograph developed from a large number of measured rainfall-runoff events in instrumented watersheds. The hydrographs derived from the actual events were first non-dimensionalized and then averaged, yielding the dimensionless curvilinear SCS unit hydrograph. Figure 4-5 shows the dimensionless SCS unit hydrograph.

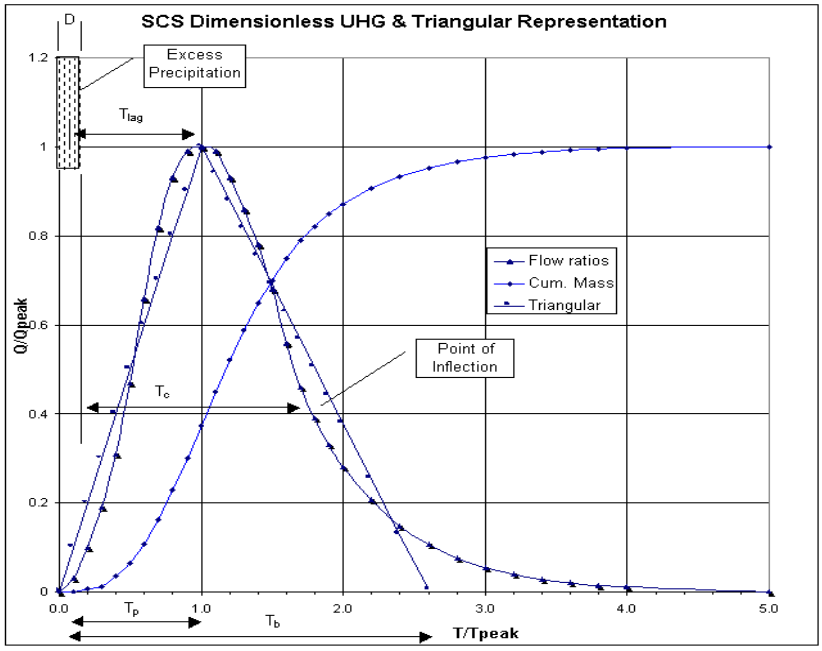

Figure 4-5: The Dimensionless SCS unit hydrograph (SCS, 1986).

The dimensionless unit hydrograph assumes that the time of concentration is the time from the end of rainfall excess to the first inflection point on the recession curve. In order to a develop relationship between the time base of the dimensionless SCS unit hydrograph and the SCS time of concentration, several relationships are needed. The first relationship concerns the time base of the dimensionless SCS unit hydrograph and the time to peak. The

time to peak is approximately one fifth of the time base of the dimensionless SCS unit hydrograph (SCS, 1972). The second relationship concerns the time of concentration to the time to peak of the dimensionless SCS unit hydrograph, which is given by the following equation:

$$t_c + D = 1.67 t_p \tag{21}$$

where t_c is time of concentration, D is duration of the rainfall excess, and t_p is time to peak. Since the time-area diagram developed within the GIS is an instantaneous unit hydrograph, the rainfall excess occurs at time zero. The relationship between the time of concentration and time to peak t_p is given by:

$$t_c = 1.67 t_p \tag{22}$$

The portion of the time base of the dimensionless SCS unit hydrograph that corresponds to the time of concentration is given by combining the observation that the time to peak is one-fifth of the time base with equation 22:

$$t_c = 1.67 t_p = 1.67 \frac{t_b}{5} = 0.33 t_b \cong \frac{t_b}{3} \tag{23}$$

where t_b is time base of the dimensionless SCS unit hydrograph.

The time-area-concentration diagram developed with the velocity method within the GIS is an IUH for which the time base equals the pixel-based time of concentration. Thus, in order to compare the t_{obs} with the pixel-based time of concentration, we have simply divided the pixel-based time of concentration by three. The time of concentration derived with this method, hereafter will be referred as SCS pixel-based time of concentration, $t_{p,scs}$.

4.2.2.2 Volume-based Time-Area Method

The time-area diagram was computed for each watershed in the study dataset, where the pixel-based time of concentration is the time-base of the time-area diagram. The first question that arose was, "What portion of the drainage area contributes to runoff at the observed time of concentration?". Figure 4-6 illustrates the answer to this question. The area under the time-area-concentration diagram for the observed time of concentration, *Vobs,* is normalized by the total area under the time-area-concentration diagram producing a dimensionless ratio between output and input. These ratios were then averaged for each physiographic region and across the state of Maryland. The average ratio represents the empirically derived value which could be used to predict the time of concentration using a time-area diagram approach.

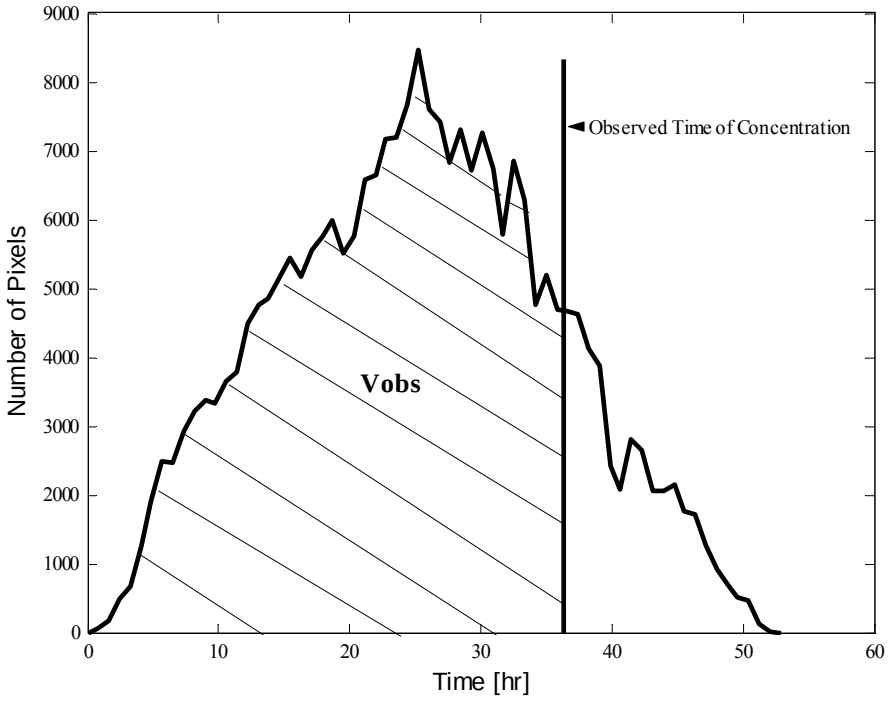

Figure 4-6: The volume under the time-area-concentration diagram corresponding to the observed time of concentration is shown as V_{obs} .

Since the observed time of concentration was used to predict the fraction of the time-area-concentration diagram that contributes runoff, the time of concentration that was calculated based on this fraction also reflects the watershed characteristics that are the integral of the time-area-concentration diagram from t=0 to t=t_{obs}. This time of concentration will be further referred as the volume-based time of concentration, t_v.

4.2.2.3 Unit Hydrograph Time-Area Method

The time-area-concentration diagram corresponds to an instantaneous unit hydrograph. In order to convert this IUH into a unit hydrograph that takes into the account the effects of storage, various alternatives can be used. A common technique is to route the IUH through a single linear reservoir (SLR). The single linear reservoir equation is given by:

$$SLR = \frac{1}{b} e^{-t/b} \tag{24}$$

where b is the routing coefficient (hrs.). Empirical evidence suggests that the routing coefficient is equal to 60 percent of the time-base of the time-area IUH (McCuen, 2005). In order to convolve the *SLR* with time-area-concentration diagram, the *SLR* needs to be evaluated over a discrete set of ordinates, such that the ordinates sum to 1.0. This is necessary to preserve the volume of IUH. The convolution technique is sensitive to the number of ordinates on the *SLR.* In order to have a systematic approach to estimate the time base of the *SLR,* the base of the *SLR* is calculated as approximately 1.8 times the t_p. This is achieved by evaluating the cumulative function of the *SLR* and assuming that the accuracy would be sufficient if 95 percent the time base of the function is considered. The cumulative *SLR* equation to predict the time base is:

$$t_b = -b \ln\left(1 - F(t)\right) \tag{25}$$

where *b* is 60 percent of the pixel-based time of concentration, while *F(t)* is set to 0.95. This yields a time base equal to 3*b*.

$$t_b = -b\ln\left(1 - F(t)\right) = -b\ln(1 - 0.95) = 3b \tag{26}$$

Since *b* is 60 percent of the pixel-based time of concentration, then the time base of the *SLR* is $1.8t_p$. The number of the ordinates on the *SLR* was thus computed by dividing $1.8t_p$ by the time increment of the time-area-concentration diagram, which equals 0.25 hr or each watershed. A set number of 10 ordinates corresponding to the first 2.5 hours of the SLR behavior were used in the convolution.

The effect of routing an IUH through a *SLR* would be to delay and lower the peak of the hydrograph and extend the time base, which simulates the effect of watershed storage. However, the amount of watershed storage depends both on the drainage area of the watershed and on the topography. A small watershed will have less storage than a large watershed; likewise, a watershed with flat topography will have more storage than a steep, mountainous one. Such watersheds thus needed to be treated differently. This can be achieved by routing the time-area-concentration diagram through a series of *SLR*s. The number of *SLR* to use was calculated based on an empirical relationship developed by Eaton (Eaton, 1954). The Eaton equation estimates the storage delay time *K* which is the ratio of the storage over the watershed and drainage area (*A* in square miles), longest path (*L* in miles) and a branching dimensionless factor *r* which varies from 1 to 2. The equation is given by:

$$K = 1.2\left(\frac{A^2}{L^2 r}\right)^{1/3} \tag{27}$$

where *L* equals 1. $35A^{0.6}$ from Singh (1989) and *r* is assumed to be 2. The *K* values calculated with this equation range from 1 to 4, which is consistent with the standard

practice.

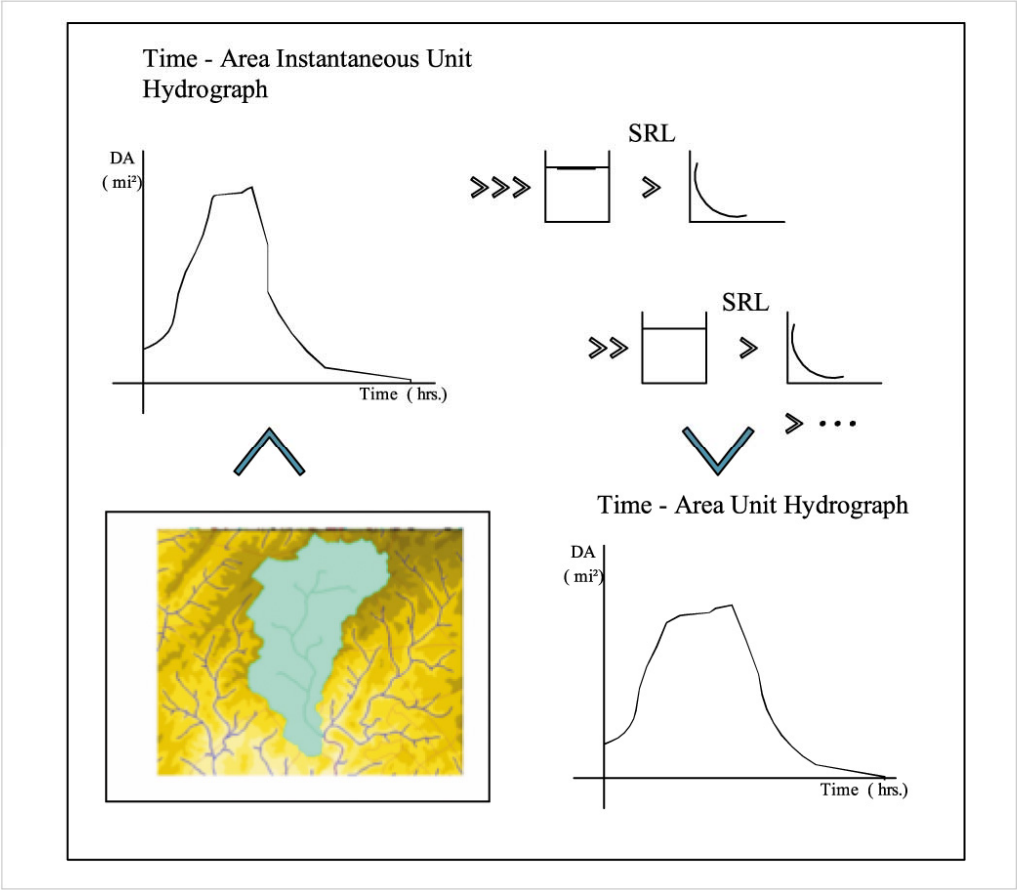

Figure 4-7: Schematic diagram of the process of routing the IUH through a series of *SLRs* to develop the time-area UH.

Figure 4-7 shows the process of the routing the IUH through a series of *SLRs* to develop the time-area unit hydrograph. The process of converting the IUH to a UH was performed to compare the two times of concentration derived from the different approaches. These times are the observed time of concentration and the time of concentration derived with the velocity method on the time-area "unit hydrograph". The duration of the rainfall excess is assumed to be the storage delay time *K* multiplied with the incremental time on the time-area-concentration diagram of 0.25 hr. Thus, the time of concentration is computed as

the time at the first inflection point on the regression curve minus the synthetic rainfall excess duration of $0.25K$:

$$t_{uh} = t_{ip} - 0.25K \tag{28}$$

This time will hereafter be referred as the unit hydrograph time of concentration, t_{uh}.

4.2.3 Time-Area Methods Results

The three time of concentration estimates that use the time-area diagram concept were calculated for each physiographic region in the state of Maryland. The GOF statistics are shown in Table 4-3. As with the gradually varied flow, *Se/Sy* represents the relative standard error of estimate between the t_c estimates and t_{obs}. Likewise, $\bar{e}/\bar{y}$ is the relative bias of t_c estimates to the t_{obs}.

Table 4-3: Time-area approach: Goodness-of-Fit statistics.

Region	GOF	The SCS pixel-based time of concentration, $t_{p,scs}$	The volume-based time of concentration, t_v	The unit hydrograph time of concentration, t_{uh}
Appalachian Plateaus region (n=17)	*Se/Sy*	0.58	0.88	2.07
	$\bar{e}/\bar{y}$	-0.17	0.21	0.80
Coastal Plain region (n=22)	*Se/Sy*	0.92	0.59	0.60
	$\bar{e}/\bar{y}$	-0.51	-0.14	-0.04
Piedmont region (n=29)	*Se/Sy*	0.99	1.00	3.26
	$\bar{e}/\bar{y}$	-0.08	0.10	1.21
State of Maryland (n=68)	*Se/Sy*	0.72	0.61	1.19
	$\bar{e}/\bar{y}$	-0.31	0.02	0.48

The computational approaches, which are used in these three methods, differ in their level of sophistication. From these results, it appears that, as the method employs a more

theoretical approach, it does not achieve greater accuracy. The SCS pixel-based time of concentration $t_{p,scs}$ is the simplest method to apply. In each region it under-predicts the observed time of concentration. In this regard, the $t_{p,scs}$ method resembles the single-segment time of concentration method. Although the *Se/Sy* may be better in some regions than for the other two methods, this method also under-predicts in all of the regions, often by a relative large amount. Likewise, the unit hydrograph time of concentration, t_{uh} in two of three physiographic regions over-predicts the observed time of concentration similar to the pixel-based time of concentration.

The volume-based time of concentration, t_v slightly over-predicts in two of three regions in state of Maryland (the Appalachian Plateaus and Piedmont region). The GOF statistics of t_v method are the best among the GOF statistics of the time-area methods; however, the t_v method *Se/Sy* values are still poor. These GOF statistics, along with statistics for all other methods considered, will be summarized in Chapter 5.

4.3 A Statistical Approach for Merging Sections along the Longest Flow Path

Increased discretization of the longest flow path in time with the velocity method as shown in the Chapter 3 does not produce more accurate estimates of the time of concentration. Figure 3-4 in Chapter 3 shows the effect of merging the pixels over the longest flow path (in time) and the time of concentration that results from merging the flow path into segments of various lengths. Is there a way to predict the number of segments to use to most accurately match the observed time of concentration? In this section, this question is addressed using a statistical approach. A regression equation will be calculated to predict the optimal number of segments to use along the longest flow path. The predictor variables will be watersheds characteristics that are readily determined using a GIS.

The predictor variables used in developing the regression equation can be classified into three groups: watershed characteristics (drainage area, percent impervious area, percent urban areas, percent forest cover), Area-based (total non-normalized area under the longest flow path, single non-normalized area under the longest flow path, integrated area), and Slope-based (25-percent frequency slope, 75-percent frequency slope, slope variation index, watershed slope, channel slope, etc.) These terms will be defined below.

Watersheds Characteristics Indices:

Watershed characteristics used in this study include the drainage area in square miles, urban areas in percent, forest cover in percent, and impervious area in percent. The land use data used in this analysis were collected from several sources. These include the GIRAS land use (USGS, 2006), Maryland Department of Planning land use from 1990, 1994, 1997 and 2000 (MDP), Zoned land use, and EPA – MRLC (Multi-Resolution land cover, 1992) depending on the availability of the data in the state of Maryland.

Area-based Indices:

Total and Single Volume Indices:

The total volume index is developed by integrating the area under the longest flow path profile where elevation in feet is the ordinate and distance in feet is the abscissa. The elevation and distance were not normalized prior to integration since some level of the correlation between the number of sections and total volume was lost. The single volume index is developed by integrating the single-segment flow path, where the slope of the flow path is determined using the overall drop in elevation divided by the overall flow length. In the same manner as with the total volume index, prior integration normalization was not

performed. Figure 4-8 shows the total volume and single volume areas for a specific example.

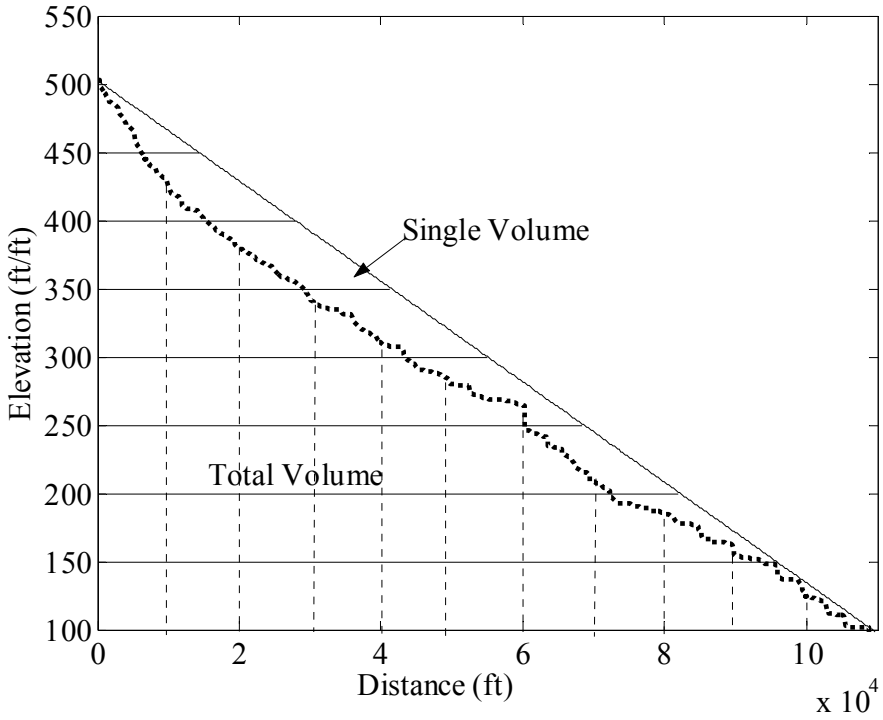

Figure 4-8: Single volume and total volume indices for one particular watershed.

Integrated area index:

The integrated area index quantifies the variation of the profile section for the channel portion of the flow by integrating the area under the flow path profile sections and subtracting it from the single segment integrated area. The single-segment integrated area equals 0.5 since, preceding the integration profiles were normalized in both relative elevation and flow length dimensions. The variable flow path profiles were first sorted by slope and then normalized in both relative elevation and flow length dimensions. This index was developed since it was observed that the greatest variation in travel times was obtained for watersheds with a longest flow path profile that have the greatest deviation from the single slope profile (Figure 4-9).

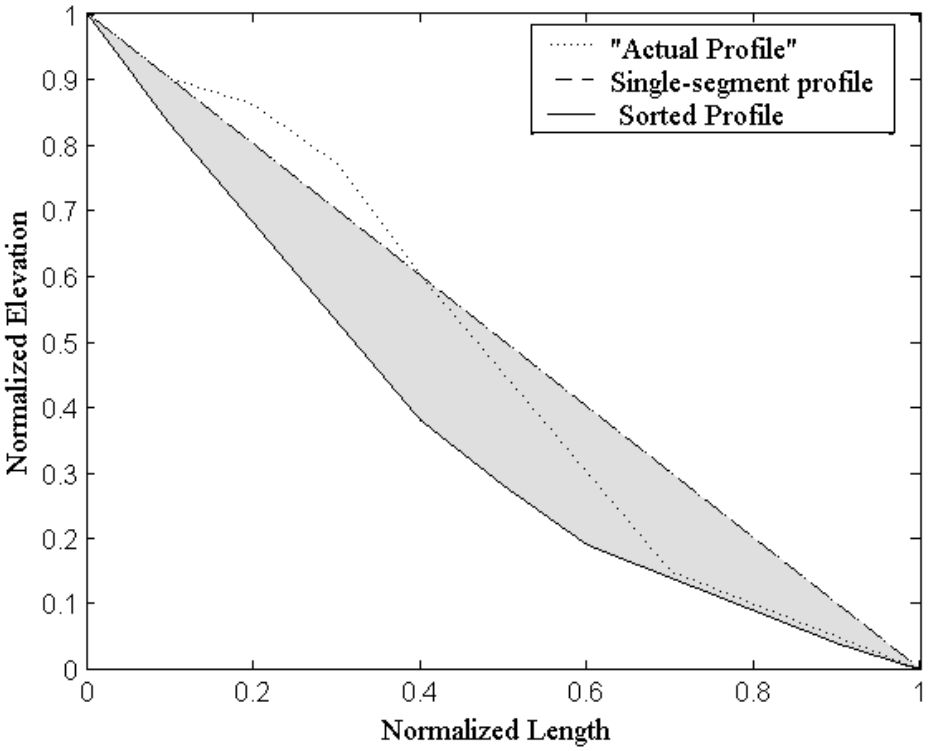

Figure 4-9: Area-based integrated area index.

Slope-based indices:

Slope-based indices capture the watershed characteristics that are not achieved with area-based indices. They are: watersheds slope, channel slope, slope variation, weighted slope, 25-percent frequency slope, 75-percent frequency slope, and flat index.

Channel Slope and Watershed Slope Indices:

Channel slope and watershed slope are indices that are commonly used in hydrology. The channel slope (feet per mile) is calculated by dividing the elevation difference between the 10^{th} and 85^{th} percent of the longest flow path by the horizontal distance between these locations. The 10^{th} and 85^{th} percent location points of the longest flow path are calculated relative to the outlet point. The watershed slope is an average land slope measured locally for each 30 meter pixel in the watershed.

Slope variation index:

The slope variation index quantifies the variation of the slope from one section (pixel) to another. This index is computed when the absolute slope difference from one section to the adjacent is summed over the watershed longest flow path. Two watersheds that have the same slopes but a different organization of these slopes will have the same value of the integrated area index since the profiles were first sorted. Thus, this index quantifies the variation of the watersheds slopes with respect to their organizations. Figure 4-10 shows an example where two flow paths, both with ten sections, have the same values of section slope values but a different sequence. The slope variations index, when calculated for these two profiles, gives values of 0.03 and 0.07. This index will be hereafter referred as the slope variation index.

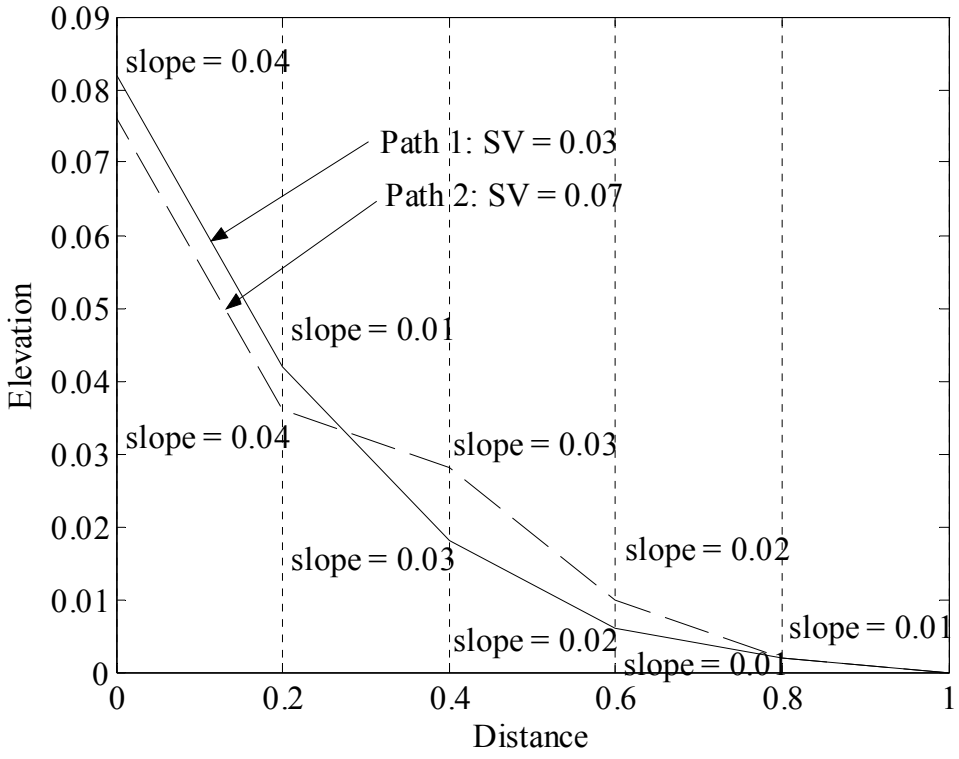

Figure 4-10: Small example of the slope variation index calculation.

Weighted slope index:

The weighted slope index is an index where the slope is multiplied by *R* (hydraulic radius) at each pixel and then summed along the longest path**.** The value at each pixel is weighted in such a way that the greatest weight is given to the upper part of the watershed and lowest weight to the pixel at the outlet. Since the swale portion of the flow, due to small hydraulic radius and small slopes, can produce the greatest values of travel time, this index tends to emphasize watersheds with the flat swales. The sum along the longest flow path is then divided by the total weight along the pixels. For example, if the flow path is divided into ten sections, the weight of the most distant pixel from the outlet will have the weight of 0.95, next 0.85 and so forth. The outlet pixels will thus have a weight of 0.5. The total weight W_t equals 5, corresponding to the sum of the weights along the longest flow path. The weighted slope index equation is:

$$WSI = \sum_{i=1}^{i=n} \frac{S_i W_i R_i}{W_t}, \quad n = number\ of\ pixels \tag{29}$$

where *S* is slope in feet per feet, *R* is hydraulic radius in feet and *W* is the weight of the pixel.

25 percent frequency index and 75 percent frequency index:

The 25 percent slope index and 75 percent slope index represent the slope values at 25 percent and 75 percent of the sorted slope range along the longest flow path. The slopes along the longest flow path are first sorted. The slope value that occurs at 25 percent from the minimum slope value represents the 25 percent slope index while the value that occurs at 75 percent represents the 75 percent slope index.

Flat Index:

The flat index (*FI)* captures the flat areas along the longest flow path. The *FI* is calculated when a length of two or more adjacent pixels with slopes less than 0.001 feet per

feet is located along the flow path. The *FI* is then divided by the total length of the channel to obtain the percentage of flow path that have flat sections (Figure 4-11). The value of 0.001 feet per feet has been arbitrarily chosen. All indexes are shown in Appendix D.

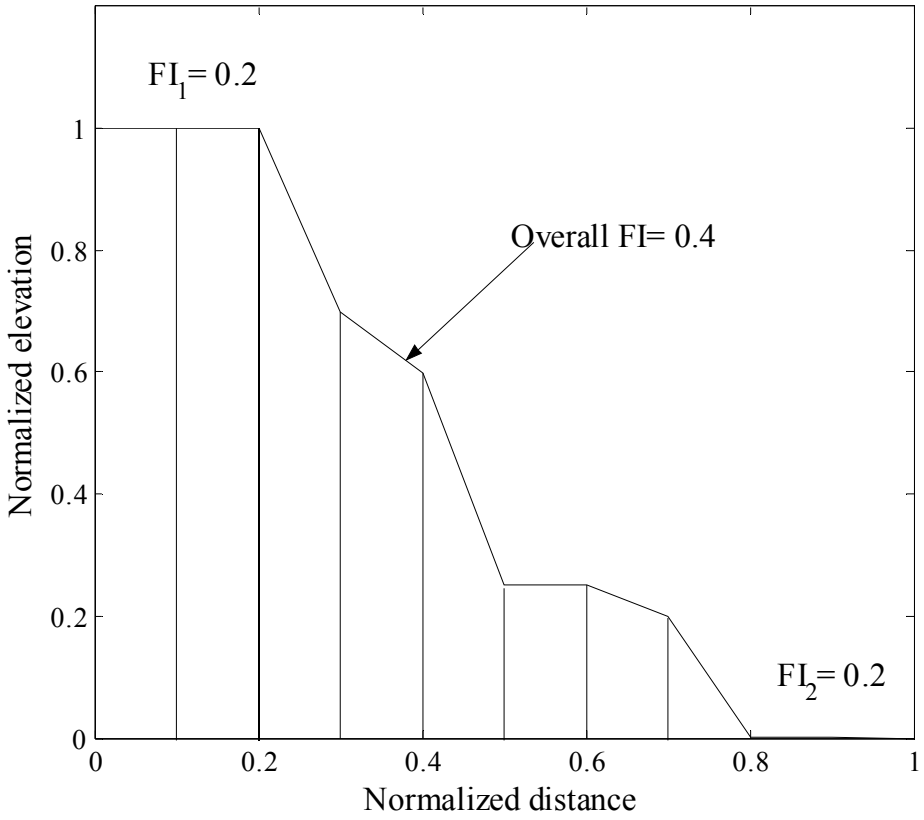

Figure 4-11: Slope-based watershed index: Flat Index.

All quantities become potential predictor variables in the regression equation calibrated using the numerical optimization program (NUMOPT, McCuen 2005). The criterion variable in this regression equation is the number of segments to use along the longest flow path. The criterion variable was developed by merging an equal number of pixels along the longest flow path and calculating the time of concentration for the merged segments. In this way, Figure 3-4 was developed for each watershed in dataset. The number of sections which gave the observed time of concentration is the criterion variable.

A stepwise regression analysis was used to evaluate which predictor variables are most significant predictors for each physiographic region in the state of Maryland. The numerical optimization program (NUMOPT, McCuen 2005) was then used to calculate the unknown regression coefficients and exponents in the power equation with the general form:

$$\#\ of\ segments = aP_1^{b_1}P_2^{b_2}P_3^{b_3}\cdots \quad (30)$$

Equations 30, 31, and 32 shows the predictor variable (*P*) and calibrated regression equation coefficient for each physiographic region in state of Maryland. The Appalachian Plateaus regression equation for predicting the number of segments along the longest flow path is:

$$\#\ of\ segments = 9.14 * FC^{2.00}CS^{1.10}WS^{-3.87}IA^{10.91}S25^{1.16}FI^{-0.205} \quad (31)$$

The Coastal Plain regression equation for predicting the number of segments along the longest flow path is:

$$\#\ of\ segments = 6.43 * DA^{1.51}UA^{-0.565}CS^{0.72}WS^{0.80}\left(TV\cdot 10^{-8}\right)^{-3.25}S25^{0.82}WeS^{6.38}FI^{7.09} \quad (32)$$

The Piedmont region regression equation for predicting the number of segments along the longest flow path is:

$$\#\ of\ segments = 4.19 * DA^{1.82}FC^{0.91}WS^{-0.47}IA^{4.14}S25^{1.66}SV^{1.46}(TV\cdot 10^{-8})^{-2.42} \quad (33)$$

where drainage area is in square miles (*DA*), urban areas is in percent (*UA*), forest cover is in percent (*FC*), watershed slope is in feet per feet (*WS*), channel slope is in feet per miles (*CS*), integrated area index is dimensionless (*IA*), 25 percent frequency index is in feet per feet (*S25*), flat index is dimensionless (*FI*), weighted slope index is in feet (*WeS*), slope variation is in square feet (*SV*), and total volume index is in square feet (*TV*).

The regression equations developed with NUMOPT may not be rational since the relationships between the predictor variables and the criterion variable are not consistent

across the regions. For example, the watershed slope index has a negative exponent in the Appalachian Plateaus and Piedmont regions while it has a positive exponent in the Coastal Plain region. Likewise, the flat index coefficient is positive in the Coastal Plain region but is negative in the Appalachian Plateaus region. Irrationality of the regression coefficients and/or exponents is attributed to high inter-correlation between the predictor variables. Predictor variables that are inter-correlated explain the same variation around the observed time of concentration which leads to irrational exponents in the regression equation. All area-based and slope-based indices are highly correlated. However, satisfactory GOF statistics were achieved only when all predictor variable were included, particularly in the Piedmont region. Despite this shortcoming, these equations are further used to predict the number of segments needed and the resulting time of concentration based on this number of segments. The time of concentration calculated utilizing the NUMOPT regression equations hereafter will be referred as the merged-segment time of concentration.

The merged-segment time of concentration was calculated using the pixel-based longest flow path. Individual pixels along this flow path were merged into segments used to calibrate the regression equations (eq.30) described above. The needed number of merged pixels was calculated by dividing the total number of pixels along the channel portion of the flow with the number of segments predicted with the regression equations for each physiographic region. The non-channel portion of the flow was treated as a single-segment. The sum of the travel time for the merged number of segments for the channel portion of the flow and the single-segment non-channel portion of the flow gives the overall merged-segment time of concentration. Appendix B shows the calibrated time of concentration for each watershed developed with the merged-segment time of concentration. The GOF

statistics for the merged-segment time of concentration for each physiographic region is shown in Table 4-7.

Table 4-7: Merged segment time of concentration Goodness-of-Fit statistics.

Region	GOF Statistics	Merged-segment Time of Concentration t_m
Appalachian Plateaus region	*Se/Sy*	0.50
	$\bar{e}/\bar{y}$	-0.02
Coastal Plain Region	*Se/Sy*	0.63
	$\bar{e}/\bar{y}$	0.01
Piedmont region	*Se/Sy*	0.75
	$\bar{e}/\bar{y}$	0.06
State of Maryland	*Se/Sy*	0.51
	$\bar{e}/\bar{y}$	0.01

The merged-segment time of concentration method performed well with respect to both the relative standard error (*Se/Sy*) and relative bias ($\bar{e}/\bar{y}$). The relative biases for each physiographic region are almost zero, indicating good predictability of the model. The relative standard error suggests that the model accuracy is moderate to good depending on the region. In the next chapter, the GOF statistics of this model will be compared to GOF statistics of the referenced model, t_r.

Chapter 5: Results and Discussion

5.1 Comparison of Proposed Methods

This study seeks to develop methods that produce accurate estimates of the time of concentration using the velocity method within a GIS environment. Model performance of several methods across three physiographic regions in Maryland was presented in Chapter 4. The Thomas et al. (2002) time of concentration method is used as a reference method, to which we compare all other methods. The SCS lag based time of concentration t_{lag} is also used as a reference method because of its common use in engineering applications.

In Chapter 4, five models for computing the time of concentration ($t_{p,scs}$, t_{uh}, t_v, $GVF_{c,p}$, and t_m) were developed. The pixel-based (t_p) and single-segment times (t_s) of concentrations, respectively, tend to greatly over-predict and under-predict t_{obs} (Figure 3-2). In the time-area analysis method ($t_{p,scs}$), the time of concentration was developed by dividing t_p by three. This is based on SCS unit hydrograph theory. This method under-predicts t_{obs} in all physiographic regions. The "time-area" t_{uh} time of concentration, based on the conversion from an instantaneous unit hydrograph to a unit hydrograph by routing through linear reservoirs, over-predicts considerably in two out of three study regions.

The time-area volume based time of concentration (t_v) is an empirically derived time, calculated by averaging the ratio of the volume under the time-area-concentration diagram at the observed time of concentration, $t_{obs.}$ Although this method has rational GOF statistics, t_r performs consistently better across all physiographic regions. The gradually varied flow estimate ($GVF_{c,p}$) uses a gradually varied flow approach for the channel portion of the flow and the pixel-based velocity method for the non-channel portion of the flow. In the majority

of the cases, $GVF_{c,p}$ provides a moderate estimate between the extremes of the pixel-based, t_p, and the single-segment times of concentration, t_s. Finally, the t_m method is based on merging the number of segments along the longest flow path. The number of segments used is based on a regression equation calibrated in this study (eq. 31-34). This method closely matches the performance of the t_r method.

The relative standard error and relative bias were calculated for each method in order to assess the prediction capacity of the models. The relative standard error of estimate (*Se/ Sy*) quantifies the sample variation of the time of concentration prediction from the t_{obs}. Values less then 0.5 of the relative standard error suggest that the method predicts the time of concentration fairly well, while values greater then 1 suggest that the prediction capacity of the method is poor. Even though the relative standard error gives a sense of the accuracy of the method, it does not indicate if the method has a systematic bias. Thus, relative bias ($\bar{e}/\bar{y}$) was calculated for each method, in order to assess whether the estimates systematically produce over- or under- prediction of t_{obs}. Table 5-1 shows the GOF statistics, *Se/Sy* and $\bar{e}/\bar{y}$, for all methods examined in this study.

Both the t_{uh} and $t_{p,scs}$ methods were excluded from further analyses since their performance is similar to the t_p and the t_s, respectively. The t_{uh} over-predicts the time of concentration in two out of three physiographic regions in the State of Maryland. The relative standard error is greater then one, in two of three physiographic regions, indicating that the estimates in these regions are poor. The $t_{p,scs\,s}$ method under-predicts t_{obs} in all regions as indicated by the negative relative biases (Table 5-1). This method performs slightly better than the single-segment approach, however it does not accurately predict the

time of concentration. Thus, only GOF statistics for t_v, $GVF_{c,p}$, and t_m models were further analyzed.

Table 5-1: Comparison of the proposed methods based on the Goodness-of-Fit statistics.

Region	*GOF Statistics*	t_r	t_{lag}	t_p	t_s	$t_{p,scs}$	$GVF_{c,p}$	t_v	t_m	t_{uh}
Appalachian Plateaus region (n=17)	*Se/Sy*	0.48	0.67	3.62	0.75	0.58	0.51	0.88	0.50	2.07
	$\bar{e}/\bar{y}$	-0.11	-0.24	1.49	-0.38	-0.17	0.10	0.21	-0.02	0.80
Coastal Plain region (n=22)	*Se/Sy*	0.54	0.79	1.08	0.96	0.92	0.62	0.59	0.63	0.60
	$\bar{e}/\bar{y}$	-0.11	-0.38	0.47	-0.52	-0.51	-0.18	-0.14	0.01	-0.04
Piedmont region (n=29)	*Se/Sy*	0.71	1.04	5.28	0.79	0.99	1.41	1.00	0.75	3.26
	$\bar{e}/\bar{y}$	0.05	0.24	1.76	-0.15	-0.08	0.44	0.10	0.06	1.21
All regions (n=68)	*Se/Sy*	0.46	0.66	2.06	0.77	0.72	0.56	0.61	0.51	1.19
	$\bar{e}/\bar{y}$	-0.07	-0.20	1.06	-0.39	-0.31	0.04	0.02	0.01	0.48

Appalachian Plateaus Region Model Performance:

The Appalachian Plateaus region consists of seventeen watersheds, with the drainage areas ranging from 1.5 to 502.3 mi^2. This region is characterized by steep topography, with a small degree of urbanized land and a high degree of forest cover. While the pixel-based t_p significantly over-predicts the time of concentration for this region (relative bias equals 1.49), the single-segment approach under-predicts the time of concentration (relative bias equals -0.38). The GOF statistics of the t_v method are rational but they are indicative of a model that is not as good as the reference model, t_r.

The models t_r, $GVF_{c,p}$, *and* t_m show comparable performance as supported by the following: (1) *Se/Sy* values for these three models were 0.48, 0.51, and 0.50, respectively, and (2) the relative bias, $\bar{e}/\bar{y}$, showed that t_r under-predicted on average by about 10 percent, $GVF_{c,p}$ over-predicted by 10 percent, and t_m had essentially no bias. The $GVF_{c,p}$ over-

estimates are likely due to a combination of drainage area and forest cover effects. Four watersheds in the Appalachian Plateaus region have drainage area smaller than 3 mi^2 and forest cover greater than 80 percent. Estimates from the $GVF_{c,p}$ method are not sensitive to land use, and, especially for the smaller watersheds, tend to be larger than the observed time of concentration, t_{obs}.

Overall, this region has the best GOF statistics across all models. The relative standard error values could be a result of the sample size for this region relative to other two. The strong GOF statistics could also be partially a result of the range in drainage areas in this region, which was greater than in the other two regions.

Coastal Plain Region Model Performance:

The Coastal Plain region consists of twenty two watersheds, with drainage areas ranging from 1.9 to 114.1 mi^2. This region is located on both sides of the Chesapeake Bay and has a primarily flat topography. The pixel-based model, t_p, shows its best performance in this region although this performance is still poor. Likewise, the single-segment model, t_s, shows its worst performance in this region, as it under-predicts the observed time of concentration by over 52 percent, on average. The t_{lag} method under-predicts the time of concentration by 38 percent. However, the drainage area threshold of 4000 acres is violated in 15 watersheds in this region. The *Se/Sy* for the seven watersheds with drainage area smaller than 4000 acres is 0.58. The t_v method *Se/Sy* value is improved compared to the Appalachian Plateaus region equaling 0.59. Also, neither systematic nor the local biases are observed for this method. Again, the t_r, $GVF_{c,p}$, and t_m methods performed similarly for this region in regards to *Se/Sy* statistics. In this region, t_r has a negative bias of 11 percent while $GVF_{c,p}$ has negative biases of 18. The t_m had essentially no bias.

Piedmont Region Model Performance:

The Piedmont region consists of twenty nine watersheds with drainage area ranging from 0.1-102 mi^2. This region generally has the poorest GOF statistics with all models. As in the other regions, the t_p method over-predicts while the t_s method under-predicts. However, the t_s method has its best performance in this region, indicating that this region has overall smaller values of t_{obs} relative to other two regions. The t_v continues its consistent but relatively poor performance in the Piedmont. The lag based t_{lag} method over-predicts the time of concentration. However, in Piedmont watersheds smaller than 4000 acres (five out of twenty nine watersheds), t_{lag} values closely match those of t_{obs}. The t_r and t_m perform equally well in this region, but with poorer overall estimates than in the other two physiographic regions. The dataset for this region consists of the greatest number of watersheds and the smallest watershed drainage area range, which may have an influence on the GOF statistics. The $GVF_{c,p}$ time of concentration method, even though with a good prediction capacity in the other two regions, performs poorly within the Piedmont region. The method produces a *Se/Sy* value greater then 1, as on average it over-predicts t_{obs} by 44 percent. This may be due to the urbanized character of the Piedmont region, since gradually varied flow cannot capture the land use characteristics of the watersheds.

Model Performance Across All Region:

Overall models t_s, $t_{p,scs}$, t_p and t_{uh} perform poorer than the other models in this study. Relative standard error of the models is generally greater than 1. Bias is also a problem with t_s, $t_{p,scs}$ under-predicting while t_p and t_{uh} over-predicts. The t_m , t_r , $GVF_{c,p}$ and t_v time of concentration models perform equally well while the t_{lag} performs moderately well even though most of the watersheds are greater than the threshold area for use of this model.

Improved GOF statistics when looking across all region's as compared to the individual regions are the result of greater sample size (68) relative to the sample sizes of each region individually, which influences both the standard error (*Se*), standard deviation (*Sy*) and sample mean ($\bar{y}$).

Based on the GOF statistics, and rationality of the models, we conclude that the gradually varied flow and the merged time of concentration methods demonstrate the strongest performance among the new methods developed in this study.

5.2 Discussion of Best Performing Models:

Although the gradually varied flow method time of concentration and the merged-segment method time of concentration predict the values of the time of concentration reasonably well, both models have limitations that need to be addressed.

Based on the GOF statistics, the best new time of concentration method for the State of Maryland is the merged-segment method. This method has consistent performance across all physiographic regions relative to the reference, t_r, model. The merged-segment time of concentration method is conceptually the same as the reference model, t_r, since both employ development of regression equations for the State of Maryland from the same dataset. The t_r method directly calculates the time of concentration, while the merged-segment time of concentration method predicts the number of segments to use on the longest flow path and then uses the uniform, bankfull flow velocity method on these computed segments. A concern when using this method is that the regression equations that predict the merged number of segments may have irrational regression coefficients due to inter-correlation among the predictor variables. Multiple predictor variables in the regression equation may explain the same sample variation around the criterion variable, which leads to the potential

irrationality of the regression coefficients. However, even with the irrationality of the regression equations, this method performed the best with respect to the GOF statistics. This method, as with any regression-based model, is only applicable to the State of Maryland, since the dataset from which the regression equations were developed was from this region.

In contrast, the gradually varied flow method is applicable irrespective of the watersheds location and does not require calibration. GOF statistics for this method in two out of three regions (Appalachian Plateaus and Coastal Plain region) indicate performance almost as good as the reference model, t_r. As apparent from Table 5-1, all models yielded the worst predictions for the Piedmont region. This is likely due to the high degree of urbanization in this region, which significantly speeds the timing of runoff for the majority of the watersheds. The average values of the t_{obs} are 5.54, 12.58 and 15.77 hours for the Appalachian Plateaus, Coastal Plain and Piedmont regions, respectively. Based on ruggedness of topography alone, the Piedmont region should have a greater average value than the Appalachian Plateaus region, as well as smaller average time of concentration value than the Coastal Plain region. Smaller average values of t_{obs} in the Piedmont region suggest that the urbanization in this region has an influence on the observed time of concentration; this is particularly relevant, given that both Washington D.C., and the Baltimore metropolitan areas are within of the Piedmont region. Since gradually varied flow analysis simulates only the mechanics of channel flow, the speeding of the runoff to streams as a consequence of urbanized areas is not captured with this method (Figure 5-1).

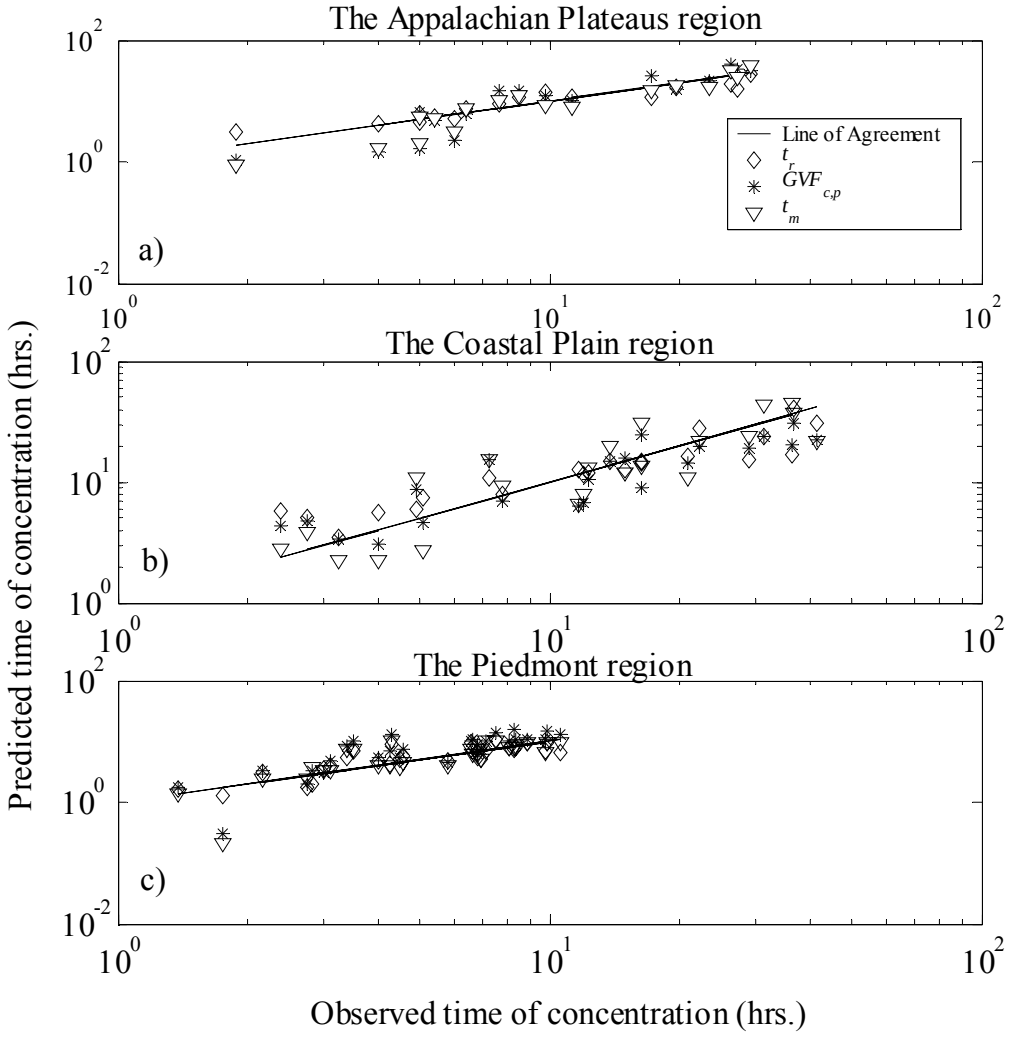

Figure 5-1: Comparison of proposed methods.

Ten out of 68 watersheds in the dataset have the t_{obs} greater then the pixel-based estimates t_p, which otherwise behave as an upper-limit to the observed t_c values. These ten watersheds are generally small (drainage area smaller than 4 mi^2), with the exception of two watersheds in Coastal Plain region with drainage areas of 7 and 18.2 mi^2. These watersheds have over 30 percent forest cover (*FC*), which may serve to delay the t_{obs} (five out of ten watersheds have *FC* greater the 80 percent). Since these watersheds are small, and thus have a small t_{obs} value, prediction error for them does not highly influence the overall model GOF

statistics. Moreover, methods that are sensitive to the watershed characteristics, such as t_r, t_m, and t_v, provide better assessment of the time of concentration in these watersheds.

The t_{obs} for 13 out of 68 watersheds was lower than the single-segment estimates, t_s, which otherwise behaves as a lower limit to the t_{obs} estimates. These watersheds have drainage areas greater then 5 mi^2 and, in general, have a high degree of urbanization. All methods poorly predict the t_{obs} for these watersheds, particularly *GVF* method. The regression-based methods, t_r and t_m are able to reduce some of the unexplained variation in t_{obs} with watershed characteristics predictors but the local relative bias is still greater then 3.

Statistical methods that relate watershed characteristics to the time of concentration performed better in the Piedmont region than did the models that simulate the hydraulics of the flow only. In Table 5-1, t_r, t_{lag}, and t_m are the statistical methods, while $GVF_{c,p}$, $t_{p,}$, t_{uh} and $t_{p,scs}$ simulate the mechanics of the flow, without relating the land use characteristics to t_c. This may explain the poorer performance of the $GVF_{c,p}$ in this region compared to the other two. Both the Appalachian Plateaus region and Coastal Plain region flow characteristics are primarily governed by the mechanics of the flow, due to the specific topography of these regions. The Coastal Plain region has a flat topography while the Appalachian Plateaus region is mountainous. In both cases, the topography is what primarily controls the timing of runoff, diminishing the importance of the effects of the land use. For example, the time of concentration is long in the Coastal Plain region due to flat topography, thus the presence of forest cover and/or urban areas will have only a secondary effect on the calculated time of concentration relative to the topography. By the same reasoning, the Appalachian Plateaus region is mountainous and the mechanics of the flow will be controlled by the steep, rugged slopes, regardless of the land use. The Piedmont region, in contrast, is not as steep nor as flat

as in the other two regions. We hypothesize that, in this region, land use plays an important role in affecting the time of concentration. Thus, any model that employs watershed characteristics has an advantage over a model that only uses topographic characteristics to simulate the mechanics of flow. To support this hypothesis, Table 5-2 shows the ranges of the drainage area, basin relief, percent urbanization and forest cover, and watersheds slope for each physiographic region.

Table 5-2: Minimum and maximum values of watershed characteristics for the 68 watersheds used in this study.

Region	Drainage Area (mi^2)	Basin relief (ft)	Urban Cover (%)	Forest Cover (%)	Watershed Slopes (ft/ft)
Appalachian Plateaus region	1.5 - 502.3	183.9-1089.9	0-14	19.8 - 95.7	0052- 0.203
Coastal Plain region	1.9-114.1	16.3-196.6	0.1-72.2	6 - 73.3	0.004 - 0.104
Piedmont region	0.1-102	110.8-379.7	0 - 77.1	2.8 - 99.2	0.047- 0.232

A comparison of basin relief between the three regions shows that the watersheds in the Coastal Plain region have overall smaller average elevation above the outlet point then other two regions. In contrast, the Appalachian Plateaus region has large values of basin relief, indicating a steep, mountainous topography. In comparison, the Piedmont region is moderate in its relief, neither as flat as the Coastal Plain, nor as rugged as the Appalachian Plateaus region. It has individual watersheds that could fit in either category, but it lacks extreme (flat and steep) topographies. Watershed characteristics that focus on land use indicate that the Appalachian Plateaus region is primarily well-forested, while Coastal Plain and Piedmont regions both have a high percentage of forest cover and urban areas. Since the Coastal Plain is low relief, land use will have a smaller effect on the timing of runoff in

comparison to the Piedmont region. Thus, we hypothesize that the better performance of the statistical methods, relative to the $GVF_{c,p}$ method are due to specific characteristics of the Piedmont physiographic region, where both the land use and the mechanics of the flow are important factors.

Both the gradually varied flow and merged-segment methods can be easily applied within the GIS, which uses high-resolution DEM data. However, the merged-segment method GOF statistics are calculated from the same dataset from which the merged segment regression-based equation (eq. 31-34) was developed. Poor predictability of the time of concentration could result from the merged-segment method when applied a watershed outside the calibrated dataset.

5.3 Model Limitations

Time of concentration is an important parameter used to predict the peak discharge and other hydrologic behavior. Many equations and models that have previously been developed reflect the numerical tools and data availability at the time of the model development. Models developed for a coarser level of data resolution may not be applicable with high-resolution GIS data. In order to accurately estimate time of concentration with high resolution GIS-based data, new methods and/or adaptation of the existing models are needed.

The time of concentration calculated using a regression approach has, for decades, been a standard practice. The new regression-based method developed in this study captures the important watershed characteristics as they vary by physiographic region to predict the time of concentration. We have developed a regression-based equation that predicts the number of segments to use along the highly discretized flow path within the GIS (eq. 31-34).

In this way, the velocity method can be adapted for high-resolution GIS data. A summary of the merged-segment method limitations are as follows:

1. The method is applicable only for watersheds with characteristics similar to the Maryland watersheds studied herein.
2. If the regression-based equations are to be applied on the watersheds outside the study dataset range, it would be necessary to recalibrate the merged-segment equations.
3. The user should be mindful that the regression equations have irrational coefficients. Although these equations estimate the time of concentration reasonably well within the study dataset, care should be used in applying them even for the watersheds located elsewhere in Maryland.
4. This method is applicable only for discretized flow paths modeled with 30 meter resolution DEM data. If other resolution data is used, the merged-segment equations would need to be recalibrated.

As opposed to the merged-segment time of concentration, the gradually varied flow method can be applied irrespective of the watershed location. The bankfull uniform flow assumption, which is part of the SCS method (SCS, 1972) recommendation, needs to be relaxed, so that the non-uniform flow along the longest flow path is modeled. In this way, both the continuity of discharge and depth will be simulated correctly. Below is a summary of the limitations of the gradually varied flow method:

1. The method is applicable only for the highly discretized flow paths, determined from 30 meter resolution DEM data and finer.

2. The method assumes gradually varied flow on the channel conveyed portion of the flow using either of the HEC-2/HEC-RAS models. Where the non-channel portion of the flow is calculated, a pixel-based approach is assuming uniform bankfull flow approach is used.
3. The method performs reasonably well with watersheds where the mechanics of the flow have the dominant effect on the timing of runoff.
4. The method may perform poorly where other watershed characteristics, such as a high degree of urbanization, have a strong influence on the timing of runoff.

Chapter 6: Conclusions

This study showed the application of GIS techniques to the NRCS velocity method for estimating the time of concentration. Using a small analytical example, we examined the discretization issue for calculating the time of concentration along the longest flow path for an idealized system. We determined velocity method time of concentration for different levels of the longest flow path discretization, where the analytical solution represents the infinitesimally small level of discretization. We showed that the time of concentration increases with the level of flowpath discretization. This suggests that automated modeling of the longest flow path by GIS techniques tends to produce larger estimates of the time of concentration, as higher resolution DEMs increase the level of flow path discretization.

We found that travel time differences result from deviations in local slope of the actual longitudinal profile from the overall average slope of the profile. The longest flow path, when modeled as a single-segment, will produce the shortest time of concentration. In contrast, the most highly discretized, pixel-based representation of the longest flow path will produce the longest time of concentration. In general, neither estimate is correct because both represent over-simplifications of the actual flow conditions in the channel. The main over-simplification in both estimates is the assumption of uniform flow at bankfull conditions. The pixel-based approach neglects issues of continuity of both discharge and flow depth while the single-segment approach, use of a reach averaged slope is generally too large to be a representative value over any appreciable flow length.

Application of single-segment and pixel-based approaches to calculating the time of concentration to a study dataset of 73 watersheds across the state of Maryland confirmed that these two methods provide under- and over-estimates of the observed travel time,

respectively. Additionally, we developed five methods for calculating the time of concentration taking advantage of high resolution GIS data and the velocity method concept. Two methods performed well based on relative standard errors and relative bias, however not without model limitations. These methods were the merged-segment method and gradually varied flow method.

We investigated if pixel-based segments could be systematically merged to produce an accurate time of concentration. This merging of segments along the longest flow path resembles traditional hydrological analysis that existed before the advent of GIS. We developed a regression equation that estimates the optimal number of segments to use based on watershed characteristics. This time of concentration, referred to as the merged-segment time of concentration, has good GOF statistics. Although, this method performed the best with respect to GOF statistics, it is recommended for use only within the state of Maryland due to the geographic coverage of the dataset used to calibrate the regression equation.

Modeling gradually varied flow conditions was found to lead to time of concentration estimates in between the bounds derived from the pixel-based and single-segment time of concentration estimates. Although uniform flow has been a standard assumption of the NRCS velocity method since its inception, our findings show that gradually varied flow modeling is needed when the flow path is highly discretized. Gradually varied flow-based times of concentration estimates were most accurate when the timing of runoff was controlled by channel hydraulics, not land use characteristics.

The time of concentration estimates calculated in this study with five different methods were compared to the observed time of concentration for each study watershed. The observed time of concentration was derived from the measured rainfall-runoff hydrograph,

where the time from the end of the rainfall excess to the first inflection point on the recession hydrograph curve represents the watershed time of concentration. These observed times of concentration do not represent the true value of the runoff timing and cannot be validated. However, these estimates are useful in quantifying the time of concentration estimates, particularly due to the availability of measured data for such a large dataset.

With greater application of GIS in watershed modeling, engineers are able to apply traditional analysis at a high level of spatial discretization. As modeling is applied on smaller increments and more detailed data, one might assume that the result would be greater accuracy. This study finds that such accuracy is not always achieved. The traditional application of the NRCS velocity method with the uniform flow assumption is not appropriate as the discretization level increases. This study finds two attractive alternative methods for estimating the time of concentration. One method employs the physics of gradually varied flow. The other strategically merges flow segments to obtain accurate estimates of the time of concentration.

Appendices

Appendix A: Excluded Watersheds From the Thomas et al. (2002) Dataset

Table A-1: Excluded watersheds from the Thomas et al. (2002) dataset.

USGS Gage Station ID	Comment
01483700	No DEM Data
01485000	Drainage Area repeated by USGS differs 24 percentages with GIS determinable drainage area.
01484548	No DEM Data
01581657	Watershed was nested within watershed 01581657.
01595000	Sub-watershed 01594930, 01594934, 01594936, 01594950 already included

Appendix B: Time of Concentration Estimates for the Study Dataset

Table B-1: Time of concentration estimates for the study dataset.

Num	ID	Region +	t_{obs} (hrs.)	t_{lag} (hrs.)	t_r (hrs.)	t_p (hrs.)	$t_{p,scs}$ (hrs.)	t_s (hrs.)	$GVF_{c,s}$ (hrs.)	$GVF_{c,p}$ (hrs.)	$GVF_{o,s}$ (hrs.)	$GVF_{o,p}$ (hrs.)	t_v (hrs.)	t_{uh} (hrs.)	t_m (hrs.)
1	01594930	A	6.38	4.66	7.40	13.39	4.46	3.85	6.30	7.00	7.12	7.82	6.39	10.75	8.42
2	01594934	A	4.00	2.00	4.20	1.77	0.59	1.07	1.48	1.53	1.60	1.65	5.54	1.25	1.73
3	01594936	A	6.00	2.30	5.00	3.14	1.05	1.25	2.32	2.34	2.98	3.00	9.01	3.25	3.12
4	01594950	A	5.00	2.30	4.40	2.00	0.67	0.96	1.70	1.70	1.78	1.78	10.35	3.75	2.00
5	01596500	A	9.75	8.20	14.30	15.74	5.25	6.29	10.58	12.52	11.47	13.41	4.80	8.75	7.74
6	01614500	A	26.33	22.70	18.80	116.56	38.85	21.49	37.32	37.32	47.75	47.75	46.54	55.50	27.87
7	01619500	A	27.12	20.40	15.50	69.99	23.33	22.89	28.24	30.06	36.42	38.24	31.60	63.25	23.82
8	01637500	A	7.62	10.50	8.80	24.24	8.08	7.29	13.61	13.65	18.21	18.25	10.70	14.25	9.64
9	01639000	A	17.25	15.50	11.30	54.21	18.07	8.45	24.46	24.47	35.05	35.06	28.15	51.50	29.48
10	01639375	A	5.00	5.80	6.30	8.82	2.94	3.43	6.46	6.51	7.08	7.13	5.21	10.75	4.95
11	01639500	A	8.50	15.70	11.80	28.54	9.51	11.46	15.17	15.22	18.68	18.73	15.01	29.25	13.94
12	01640965	A	1.88	1.90	3.00	0.90	0.30	0.73	0.95	0.97	1.04	1.06	0.67	1.25	0.80
13	01641000	A	5.44	5.70	5.40	5.24	1.75	2.64	3.99	4.05	4.69	4.75	0.48	7.00	4.72
14	03075500	A	23.50	9.10	18.80	59.13	19.71	14.97	19.26	21.02	26.18	27.94	28.76	32.75	15.60
15	03076500	A	29.25	18.00	27.80	85.15	28.38	12.97	29.02	30.76	37.91	39.66	40.64	67.75	30.27
16	03076600	A	11.25	6.30	11.50	14.73	4.91	5.12	9.61	10.14	11.20	11.73	4.86	10.00	7.42
17	03078000	A	19.58	11.50	16.80	28.22	9.41	8.28	15.11	15.44	19.38	19.71	9.48	14.75	17.27
18	01483200	CP	11.67	6.40	12.70	8.68	2.89	4.38	5.53	6.34	5.96	6.77	5.38	9.00	6.61

Table B-1: Time of concentration estimates for the study dataset (continued).

Num	ID	Region +	t_{obs} (hrs.)	t_{lag} (hrs.)	t_r (hrs.)	t_p (hrs.)	$t_{p,scs}$ (hrs.)	t_s (hrs.)	$GVF_{c,s}$ (hrs.)	$GVF_{c,p}$ (hrs.)	$GVF_{o,s}$ (hrs.)	$GVF_{o,p}$ (hrs.)	t_v (hrs.)	t_{uh} (hrs.)	t_m (hrs.)
19	01484000	CP	20.85	14.40	16.10	23.58	7.86	8.63	13.97	14.47	19.18	19.68	11.52	14.50	10.96
20	01484500	CP	14.88	12.70	12.80	23.55	7.85	11.31	15.70	15.73	21.19	21.22	13.59	8.50	11.81
21	01485500	CP	41.75	35.60	30.60	48.46	16.15	17.55	19.18	22.16	31.19	34.17	29.69	27.75	21.50
22	01491000	CP	36.88	30.70	40.60	76.20	25.40	21.89	24.84	30.68	42.62	48.46	50.64	49.50	36.60
23	01493000	CP	22.25	14.40	27.60	27.75	9.25	13.90	15.33	19.44	16.19	20.30	15.61	19.25	21.92
24	01493500	CP	16.38	8.70	14.50	40.15	13.38	10.21	16.27	24.24	27.21	35.18	21.39	14.75	30.27
25	01581658	CP	4.92	4.50	5.90	13.13	4.38	3.23	6.63	8.57	10.14	12.07	7.93	11.50	10.98
26	01585100	CP	2.75	3.60	5.00	7.07	2.36	2.88	4.37	4.75	5.40	5.78	4.21	7.00	3.85
27	01585105	CP	4.00	2.70	5.60	3.69	1.23	2.01	2.81	3.03	3.20	3.42	2.49	5.25	2.25
28	01585300	CP	2.38	3.20	5.80	5.97	1.99	2.84	3.92	4.40	4.43	4.91	3.77	6.25	2.80
29	01585400	CP	3.25	1.80	3.50	3.84	1.28	1.87	2.00	3.35	2.27	3.63	2.21	3.50	2.24
30	01589512	CP	7.75	8.20	7.90	11.31	3.77	3.83	6.84	6.87	9.57	9.59	6.39	10.00	9.18
31	01590500	CP	11.94	3.50	11.40	9.23	3.08	4.26	5.46	6.73	6.84	8.11	4.93	7.50	7.97
32	01594526	CP	36.38	9.60	16.80	52.87	17.62	12.57	19.52	20.48	27.49	28.45	31.32	31.00	45.40
33	01594670	CP	12.33	4.00	12.00	15.56	5.19	4.36	9.36	10.62	16.85	18.11	9.65	13.50	13.08
34	01594710	CP	5.08	4.30	7.30	5.77	1.92	2.67	3.30	4.62	3.84	5.15	3.32	6.50	2.69
35	01649500	CP	7.25	8.30	10.70	18.30	6.10	6.49	15.36	15.47	19.05	19.16	12.00	18.75	15.35
36	01653600	CP	29.05	9.50	15.30	29.58	9.86	11.25	14.04	19.30	16.10	21.36	12.94	14.75	23.99
37	01660920	CP	31.25	16.80	23.50	52.70	17.57	12.47	22.08	23.52	31.87	33.30	27.09	25.50	43.14
38	01661050	CP	16.38	6.60	14.80	14.99	5.00	5.73	7.81	8.85	10.06	11.10	8.95	11.00	13.44

Table B-1: Time of concentration estimates for the study dataset (continued).

Num	ID	Region +	t_{obs} (hrs.)	t_{lag} (hrs.)	t_r (hrs.)	t_p (hrs.)	$t_{p,scs}$ (hrs.)	t_s (hrs.)	$GVF_{c,s}$ (hrs.)	$GVF_{c,p}$ (hrs.)	$GVF_{o,s}$ (hrs.)	$GVF_{o,p}$ (hrs.)	t_v (hrs.)	t_{uh} (hrs.)	t_m (hrs.)
39	01661500	CP	13.75	8.60	15.00	27.07	9.02	6.41	9.42	14.97	13.06	18.61	18.95	22.00	19.58
40	01495000	P	8.88	10.80	9.50	16.69	5.56	9.29	10.63	10.97	11.87	12.21	7.40	19.00	9.72
41	01496200	P	5.81	4.50	4.80	8.27	2.76	3.38	4.83	4.64	6.39	6.20	3.27	8.25	3.95
42	01580000	P	7.50	11.80	11.00	28.67	9.56	9.15	13.15	13.62	16.75	17.22	12.06	18.50	10.78
43	01581700	P	3.50	9.70	7.10	17.85	5.95	6.10	10.38	10.41	14.01	14.04	5.78	14.25	7.22
44	01582000	P	6.62	7.90	7.00	19.06	6.35	5.46	10.09	11.11	13.98	15.00	7.86	14.00	6.44
45	01583100	P	4.50	5.20	5.00	10.23	3.41	3.17	5.19	5.43	6.62	6.86	4.74	10.25	3.58
46	01583500	P	8.08	9.30	8.10	20.15	6.72	5.83	10.21	10.45	13.14	13.38	8.93	16.25	9.21
47	01583600	P	4.25	5.30	4.30	11.52	3.84	3.48	6.72	6.85	9.75	9.88	4.42	8.75	4.03
48	01584050	P	3.00	3.60	3.60	5.05	1.68	1.90	2.96	3.07	3.68	3.79	2.94	6.25	3.41
49	01585200	P	1.38	1.70	1.60	2.49	0.83	1.23	1.52	1.72	1.92	2.12	1.14	3.75	1.23
50	01585500	P	3.12	3.00	4.00	5.82	1.94	2.11	2.35	4.70	2.75	5.10	2.10	6.00	2.76
51	01586000	P	9.75	8.60	6.90	17.56	5.85	5.81	8.56	10.81	10.58	12.83	8.78	19.00	7.13
52	01586210	P	4.00	6.30	4.80	7.41	2.47	3.70	4.92	5.35	5.86	6.29	3.34	8.75	4.13
53	01586610	P	4.58	7.70	5.80	12.86	4.29	4.06	6.24	7.27	7.91	8.94	5.48	12.75	4.46
54	01589100	P	2.17	2.30	3.00	4.33	1.44	1.78	2.33	3.37	3.03	4.07	1.81	5.00	2.20
55	01589300	P	3.38	7.90	5.50	17.53	5.84	6.28	7.27	8.34	8.40	9.47	7.72	17.00	7.37
56	01589330	P	2.83	2.30	2.00	5.69	1.90	2.23	2.91	3.32	3.71	4.12	2.84	6.75	2.41
57	01589440	P	6.92	6.00	5.00	12.53	4.18	3.94	5.30	7.40	6.51	8.61	5.46	13.00	6.09
58	01591000	P	7.12	7.50	7.10	16.71	5.57	4.73	9.59	9.96	13.82	14.19	7.45	11.00	9.27

Table B-1: Time of concentration estimates for the study dataset (continued).

Num	ID	Region +	t_{obs} (hrs.)	t_{lag} (hrs.)	t_r (hrs.)	t_p (hrs.)	$t_{p,scs}$ (hrs.)	t_s (hrs.)	$GVF_{c,s}$ (hrs.)	$GVF_{c,p}$ (hrs.)	$GVF_{o,s}$ (hrs.)	$GVF_{o,p}$ (hrs.)	t_v (hrs.)	t_{uh} (hrs.)	t_m (hrs.)
59	01591400	P	6.83	5.60	5.50	8.81	2.94	3.33	5.25	6.31	6.49	7.55	4.26	9.75	6.86
60	01591700	P	6.83	8.00	6.40	16.94	5.65	4.97	8.18	9.08	11.35	12.25	6.18	10.00	5.90
61	01593500	P	10.58	9.90	6.70	25.81	8.60	7.77	12.42	13.22	17.12	17.92	13.60	18.00	9.57
62	1593710	P	8.25	9.70	7.30	36.93	12.31	6.45	15.42	15.86	24.53	24.96	14.28	23.25	6.39
63	01594000	P	9.88	13.70	9.70	48.89	16.30	9.05	14.66	15.05	19.85	20.24	7.71	27.50	8.93
64	01643495	P	1.75	0.40	1.30	0.21	0.07	0.19	0.30	0.30	0.35	0.35	0.03	0.21	0.21
65	01643500	P	8.35	8.70	8.10	19.87	6.62	6.03	10.87	11.04	14.20	14.37	7.35	15.00	8.99
66	01645000	P	4.31	12.10	8.70	26.97	8.99	7.94	13.18	13.41	17.00	17.23	11.32	22.25	10.36
67	01645200	P	2.75	2.20	1.80	2.51	0.84	1.59	1.81	2.00	2.07	2.26	1.15	3.75	2.34
68	01651000	P	6.58	10.30	9.50	24.31	8.10	7.74	10.38	10.47	13.55	13.64	10.52	12.75	7.60

* watersheds excluded from the dataset based on the 7 hrs. single-segment swale portion of the flow
+ Regions are: Appalachian Plateau (AP), Piedmont (P) and Coastal Plain (CP)
** Watersheds with USGS ID 01484100, 01486000, 0148700, 0148850, and 0148900 excluded based on 7 hrs. non-channel portion of the flow criterion.

Appendix C: HEC-2 Input File

The gradually varied flow analysis was calculated with HEC-2/HEC-RAS programs for the channel portion of the longest flow path. We simulated the steady non-uniform flow regime for the sub-critical flow condition. The sub-critical flow condition assumes that the depth of the channel is greater than the critical depth achieved for the minimal specific energy of the flow. The sub-critical flow condition requires a downstream boundary condition in order to perform the calculation of the water surface profile and, thus, the channel travel time. In this case, the boundary condition represents the channel slope at the outlet pixel. When the flow depth in the section is less than the critical depth, this analysis will assign the critical depth to super-critical flow sections.

In addition to the flow regime and its boundary conditions, the HEC-2/HEC-RAS input file requires both the channel profile, as well as the cross-sectional profile information. The channel characteristics include: channel section (i), incremental length between sections (dx), Manning's roughness number (n) and cross-section profile. This information is calculated within the GIS along the longest flow path. For each pixel along the longest flow path the drainage area is determined, the elevation at the beginning and the end of the pixel (30 meter resolution DEM data), the cross-sectional width at mid-pixel (U.S. Fish and Wildlife Service (McCandless and Everett, 2002; McCandless, 2003a and 2003b)) and incremental length between the sections (30 or $30\sqrt{2}$ meters) within the GIS (Figure C-1). The cross-sectional shape is assumed to be rectangular along the channel, while Manning's roughness number equals to 0.05 for the channel and 0.1 for the overbank flow.

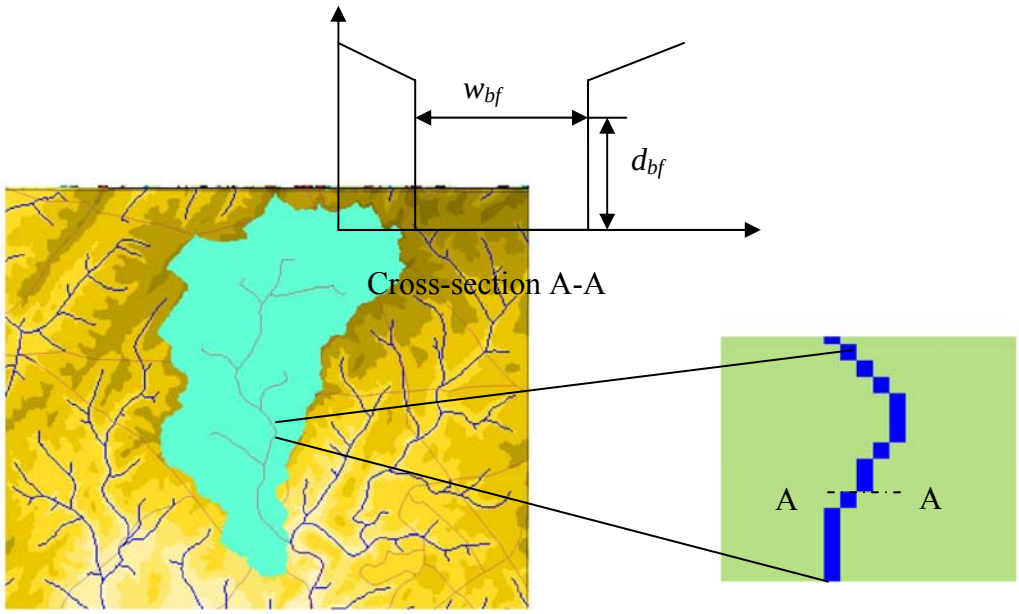

Figure C-1: Cross-section illustration for one pixel section.

The HEC-2 file is in a restrictive format, such that first column (field) in the file is two characters wide, the second column is six characters wide, and every remaining column is 8 characters wide. The first column of the HEC-2 input file is a “character card”, found at the beginning of each line (field 0), defining the content of the line. Table C-1 shows the “character card” used in the GVF analysis input file, generated for the longest flow path.

Table C-1: HEC-2 input "character card" description generated for this *GVF* analysis.

HEC-2 input file "character card"	*Description*
AC	Saves the computer readable output file from the HEC-2/HEC-RAS.
T1/T2/T3	Document cards, available for the text within the record
J1	Starts the new record
J3	Defines the steady flow with its characteristics
NC	Defines the Manning's n coefficient
X1	Defines cross-section information
X2	Change discharge at section
GR	Cross-section characteristics: channel cross section elevation and width
EJ	End Job
ER	End Record

An example of the HEC-2/HEC-RAS input is shown in Figure C-2. Each field in each "characteristic card" has pre-specified information requirements. Tables C-2, C-3, C-4, and C-5 explain the field requirements for J1, J3, NC, and X1 "cards", respectively. Only information used in gradually varied flow analysis are shown in the tables. Any further information about the HEC-2 input file can be found directly in the HEC-2 documentation.

```
AC
T1     HEC-2 input file for HEC-RAS
T2     Stream reach with n cross-section
T3     Arc-View generated cross-section for the longest path
J1   -10                    0.000.000526    0.00
J3    38      39       6      26      14      43       7       8      25      68
NC  0.10    0.10    0.05     0.1     0.3
X1   1.0     8.0   500.0   557.5     0.0     0.0     0.0
X21194.8
GR 366.3    0.00   361.3   500.0   357.4   500.0   357.4   528.8   357.4   543.1
GR 357.4   557.5   361.3   557.5   366.3  1057.5
X1   2.0     8.0   500.0   557.5    98.4    98.4    98.4
X21194.8
GR 366.4    0.00   361.4   500.0   357.5   500.0   357.5   528.8   357.5   543.1
GR 357.5   557.5   361.4   557.5   366.4  1057.5
X1   3.0     8.0   500.0   557.5   139.2   139.2   139.2
X21194.3
GR 366.4    0.00   361.4   500.0   357.6   500.0   357.6   528.8   357.6   543.1

                    omitted section

X1 585.0     8.0   500.0   513.4    98.4    98.4    98.4
X2  69.3
GR 641.5    0.00   636.5   500.0   635.4   500.0   635.4   506.7   635.4   510.0
GR 635.4   513.4   636.5   513.4   641.5  1013.4
X1 586.0     8.0   500.0   513.3    98.5    98.5    98.5
X2  69.3
GR 641.5    0.00   636.5   500.0   635.5   500.0   635.5   506.7   635.5   510.0
GR 635.5   513.3   636.5   513.3   641.5  1013.3
X1 587.0     8.0   500.0   513.3    98.4    98.4    98.4
X2  68.6
GR 641.6    0.00   636.6   500.0   635.5   500.0   635.5   506.7   635.5   510.0
GR 635.5   513.3   636.6   513.3   641.6  1013.3
X1 588.0     8.0   500.0   513.3    98.4    98.4    98.4
X2  68.6
GR 641.6    0.00   636.6   500.0   635.6   500.0   635.6   506.6   635.6   510.0
GR 635.6   513.3   636.6   513.3   641.6  1013.3

EJ

ER
```

Figure C-2: Example of the HEC-2/HEC-RAS input file, based on a single watershed.

Table C-2: Field description for the HEC-2 input file for the J1 "character card."

Field	*Value*	*Description*
0	J1	Defines the job flow regime, boundary conditions and print options
1	-10	Do not print
4	0	Defines the sub-critical flow
5	Channel slope of the outlet section, simulating the water surface slope at outlet	Boundary condition at the outlet: needed for sub-critical flow
6	0	English units

Table C-3: Field description for the HEC-2 input file for the J3 "character card."

Field	*Value*	*Description*
0	J3	Specifies the output format
1	38	Section id
2	39	Length between sections
3	6	Travel time for each section
4	26	Channel velocity
5	14	Channel conveyed discharge
6	43	Discharge
7	7	Velocity
8	8	Depth
9	25	Cross-sectional area

Table C-4: Field description for the HEC-2 input file for the NC "character card."

Field	*Value*	*Description*
0	NC	Defines the Manning's roughness number and contraction coefficient
1	0.1	Manning's roughness *n* for the left overbank
2	0.1	Manning's roughness *n* for the left overbank
3	0.05	Manning's roughness *n* for the left overbank
4	0.1	Contraction coefficient
5	0.3	Expansion coefficient

Table C-5: Field description for the HEC-2 input file for the X1 "character card."

Field	*Value*	*Description*
0	X1	Specifies the output format
1	*	Section ID from the outlet
2	8	Number of points that defines the cross-section profile
3	*	Elevation at the left bank
4	*	Elevation at the right bank
5	*	Distance from the left bank to the next downstream section
6	*	Distance from the right bank to the next downstream section
7	*	Channel distance to the next downstream section

* unique values for each cross-section

The X2 “card” defines the change in discharge at each section and was calculated using U.S. Fish and Wildlife Service regional equations (McCandless and Everett, 2002; McCandless, 2003a and 2003b), which relate bankfull discharge to the drainage area. The GR “card” defines the cross-sectional profile points. Field 1 in the GR “card” contains the first elevation point from left to right, while second field contains the station coordinate for the first point, and so forth. The elevation and station information for each pixel along the longest flow path were defined with DEM data and U.S. Fish and Wildlife Service regional equation (McCandless and Everett, 2002; McCandless, 2003a and 2003b), which relate drainage area to the cross-section width for that specific pixel along the longest flow path. X1, X2 and GR “cards” need to be defined with each new pixel along the channel portion of the longest flow path generated within the GIS. At the end of the input file, ER and EJ indicate that both the task and the overall job are complete, and that the output file is should be executed.

Appendix D: U.S. Geological Survey Gaging Stations and Watershed Characteristics

Table D-1: U.S. Geological Survey gaging stations and watershed characteristics.

ID	Region	Urban Area (%)	Imper. Area (%)	USGS DA (mi^2)	GIS DA (mi^2)	Forest Cover (%)	Slope watershed (ft/ft)	Slope channel (ft/mi)	Integrated Area (/)	Total Volume (ft^2)	Single Volume (ft^2)	Slope variation Index (ft/ft)	25 % Slope (ft/ft)	75 % Slope (ft/ft)	Weighted Slope (ft)	Flat Index (/)
01594930	A	0.00	0.70	8.23	8.20	85.90	0.155	80.70	0.42262	3.90E+05	4.49E+05	0.26	0.00006	0.00076	0.00292	0.786
01594934	A	0.00	0.00	1.55	1.50	82.30	0.129	167.20	0.26867	4.61E+05	5.29E+05	0.63	0.00368	0.02299	0.01104	0.144
01594936	A	0.00	0.30	1.91	1.90	88.70	0.144	187.70	0.30339	8.58E+05	1.05E+06	1.20	0.00213	0.02337	0.01492	0.139
01594950	A	0.00	0.00	2.3	2.40	81.80	0.130	217.90	0.26074	2.41E+06	3.37E+06	2.26	0.00565	0.06753	0.02917	0.055
01596500	A	2.70	0.80	49.1	48.60	76.50	0.203	62.50	0.35432	5.12E+07	5.12E+07	7.83	0.00111	0.01029	0.01733	0.187
01614500	A	3.80	2.50	494	502.30	35.70	0.100	9.20	0.42575	9.53E+07	2.34E+08	6.84	0.00009	0.00151	0.00851	0.647
01619500	A	6.10	3.60	281	208.80	24.50	0.082	11.10	0.41485	4.08E+07	5.93E+07	3.20	0.00011	0.00086	0.00646	0.769
01637500	A	9.50	3.30	66.9	67.30	45.90	0.124	45.60	0.34587	4.61E+07	8.11E+07	6.57	0.00042	0.01365	0.02025	0.370
01639000	A	2.30	1.30	173	172.70	19.80	0.052	19.50	0.40114	3.66E+07	1.12E+08	6.86	0.00015	0.00508	0.01493	0.527
01639375	A	1.60	5.10	41.3	38.80	67.90	0.158	73.90	0.32408	1.91E+07	3.08E+07	6.19	0.00124	0.02083	0.02499	0.186
01639500	A	11.10	3.40	102	103.00	23.60	0.081	12.10	0.37362	2.17E+07	3.27E+07	2.83	0.00040	0.00203	0.00796	0.601
01640965	A	1.40	0.40	2.14	2.20	95.70	0.163	326.20	0.17811	3.04E+06	3.54E+06	2.96	0.02730	0.07856	0.04137	0.010
01641000	A	14.00	5.90	18.4	19.10	72.70	0.127	136.50	0.30151	2.85E+07	3.27E+07	7.91	0.00488	0.03146	0.03508	0.052
03075500	A	2.70	1.40	134	134.30	53.60	0.115	9.30	0.42921	4.86E+06	5.65E+06	0.95	0.00003	0.00046	0.00240	0.864
03076500	A	1.80	1.50	295	294.10	63.20	0.112	18.50	0.44021	1.60E+08	1.09E+08	6.25	0.00007	0.00145	0.00962	0.725
03076600	A	7.30	2.50	48.9	49.00	61.30	0.168	61.60	0.32586	4.72E+07	3.88E+07	6.13	0.00131	0.01524	0.01712	0.229
03078000	A	0.40	0.40	62.5	63.70	73.70	0.101	29.70	0.38234	2.54E+07	2.59E+07	3.40	0.00020	0.00441	0.00998	0.530
01483200	CP	3.20	1.20	3.85	4.20	42.20	0.016	14.60	0.35264	3.36E+05	2.83E+05	0.21	0.00035	0.00212	0.00197	0.660
01484000	CP	2.20	0.90	13.6	12.50	36.00	0.006	7.10	0.37641	6.19E+05	5.53E+05	0.26	0.00006	0.00102	0.00103	0.720
01484500	CP	10.00	6.80	5.24	4.80	38.10	0.005	5.90	0.39741	2.85E+05	2.56E+05	0.17	0.00009	0.00030	0.00067	0.816
01485500	CP	3.80	1.60	44.9	45.00	73.30	0.004	2.80	0.40199	1.17E+06	1.06E+06	0.25	0.00006	0.00020	0.00079	0.867
01491000	CP	2.80	1.20	113	114.10	37.20	0.006	3.40	0.42038	2.39E+06	2.61E+06	0.36	0.00003	0.00023	0.00120	0.905
01493000	CP	1.60	0.60	19.7	20.20	19.70	0.009	10.87	0.37844	8.45E+05	8.43E+05	0.33	0.00009	0.00090	0.00195	0.778

Table D-1: U.S. Geological Survey gaging stations and watershed characteristics (continued).

ID	Region	Urban Area (%)	Imper. Area (%)	USGS DA (mi^2)	DA (mi^2)	Forest Cover (%)	Slope watershed (ft/ft)	Slope channel (ft/mi)	Integrated Area (/)	Total Volume (ft^2)	Single Volume (ft^2)	Slope variation Index (ft/ft)	25 % Slope (ft/ft)	75 % Slope (ft/ft)	Weighted Slope (ft)	Flat Index (/)
01493500	CP	1.60	0.80	12.7	12.00	8.50	0.010	9.10	0.44390	4.73E+05	5.52E+05	0.28	0.00003	0.00072	0.00244	0.788
01581658	CP	29.50	18.70	5.22	5.20	41.20	0.038	64.20	0.36742	6.12E+05	1.06E+06	0.82	0.00005	0.00919	0.00906	0.409
01585100	CP	71.20	40.90	7.61	7.50	15.70	0.061	51.90	0.34527	2.92E+06	4.07E+06	1.97	0.00075	0.00914	0.01167	0.257
01585105	CP	35.00	16.30	2.65	2.60	33.20	0.053	63.20	0.33718	9.45E+05	1.21E+06	1.18	0.00112	0.01293	0.01279	0.208
01585300	CP	58.40	31.00	4.46	4.50	22.20	0.060	63.00	0.32729	2.09E+06	2.81E+06	1.53	0.00123	0.01574	0.01346	0.186
01585400	CP	72.70	52.20	1.97	1.90	18.90	0.035	35.30	0.28985	8.72E+04	8.78E+04	0.24	0.00080	0.00813	0.00394	0.414
01589512	CP	61.50	37.20	8.24	8.70	24.30	0.026	24.70	0.37170	1.76E+06	2.58E+06	0.95	0.00034	0.00595	0.00462	0.510
01590500	CP	16.30	5.40	6.92	7.00	61.20	0.104	24.50	0.36340	9.46E+05	8.62E+05	0.51	0.00055	0.00351	0.00341	0.590
01594526	CP	63.10	35.90	89.7	89.10	6.00	0.050	7.00	0.41482	4.19E+06	5.23E+06	0.80	0.00003	0.00096	0.00263	0.784
01594670	CP	16.60	5.90	9.38	9.30	65.00	0.085	20.10	0.34299	5.18E+05	7.34E+05	0.51	0.00012	0.00287	0.00402	0.415
01594710	CP	26.30	13.50	3.26	3.60	47.50	0.055	46.20	0.31311	6.55E+05	7.23E+05	0.62	0.00124	0.01150	0.00649	0.168
01649500	CP	66.60	39.60	72.8	73.50	6.40	0.054	27.30	0.32120	1.28E+07	1.65E+07	2.78	0.00059	0.00584	0.01047	0.320
01653600	CP	56.10	25.90	39.5	39.80	9.40	0.051	16.80	0.37651	6.98E+06	7.33E+06	1.77	0.00029	0.00216	0.00550	0.611
01660920	CP	16.50	7.20	79.9	81.00	58.10	0.032	10.70	0.39428	6.80E+06	8.62E+06	1.11	0.00004	0.00144	0.00384	0.692
01661050	CP	14.50	4.20	18.5	18.20	48.10	0.047	15.00	0.36244	1.64E+06	2.10E+06	0.77	0.00022	0.00359	0.00379	0.555
01661500	CP	42.90	19.80	24	25.20	46.80	0.025	14.60	0.37932	2.18E+06	2.00E+06	0.86	0.00018	0.00183	0.00288	0.608
01495000	P	5.30	3.70	52.6	53.30	13.90	0.073	17.50	0.31997	2.18E+07	2.51E+07	2.79	0.00065	0.00394	0.01019	0.336
01496200	P	13.10	3.80	9.03	9.00	15.70	0.052	29.00	0.33139	2.97E+06	2.81E+06	1.10	0.00076	0.00714	0.00652	0.370
01580000	P	1.40	0.80	94.4	94.30	26.80	0.102	17.90	0.39070	2.73E+07	4.03E+07	4.12	0.00021	0.00271	0.01242	0.529
01581700	P	17.00	8.50	34.8	34.60	22.30	0.070	29.90	0.35725	2.16E+07	2.29E+07	3.55	0.00070	0.00540	0.00945	0.408
01582000	P	3.90	6.40	52.9	53.80	21.70	0.103	33.40	0.36087	9.07E+06	1.25E+07	2.71	0.00027	0.00665	0.01666	0.412
01583100	P	8.20	3.80	12.3	12.40	30.80	0.083	50.90	0.38167	5.89E+06	7.53E+06	2.46	0.00054	0.00547	0.01470	0.343
01583500	P	10.80	3.40	59.8	60.30	32.50	0.082	26.10	0.39245	1.23E+07	2.10E+07	3.07	0.00038	0.00349	0.01273	0.438
01583600	P	52.60	24.50	20.9	20.90	23.50	0.076	46.00	0.35346	7.50E+06	8.93E+06	2.41	0.00038	0.01011	0.01345	0.375
01584050	P	20.30	6.20	9.4	9.20	16.90	0.066	54.10	0.33621	2.28E+06	3.27E+06	1.73	0.00085	0.01581	0.01337	0.244
01585200	P	77.10	43.00	2.13	2.20	2.80	0.059	61.60	0.29571	6.09E+05	4.96E+05	0.64	0.00102	0.02088	0.00847	0.223

Table D-1: U.S. Geological Survey gaging stations and watershed characteristics (continued).

ID	Region	Urban Area (%)	Imper. Area (%)	USGS DA (mi^2)	DA (mi^2)	Forest Cover (%)	Slope watershed (ft/ft)	Slope channel (ft/mi)	Integrated Area (/)	Total Volume (ft^2)	Single Volume (ft^2)	Slope Variation Index (ft/ft)	25 % Slope (ft/ft)	75 % Slope (ft/ft)	Weighted Slope (ft)	Flat Index (/)
01585500	P	23.30	7.90	3.29	3.30	18.70	0.081	39.10	0.34957	2.00E+05	1.30E+05	0.24	0.00014	0.00670	0.00327	0.442
01586000	P	25.00	10.10	56.6	56.00	23.00	0.081	28.10	0.40201	9.96E+06	1.01E+07	2.04	0.00038	0.00195	0.01061	0.569
01586210	P	37.90	12.30	14	14.10	21.50	0.079	45.20	0.32337	7.05E+06	7.26E+06	2.12	0.00132	0.00627	0.01261	0.178
01586610	P	18.70	5.00	28	28.00	32.30	0.089	35.40	0.37534	5.91E+06	6.80E+06	1.73	0.00018	0.00484	0.01146	0.392
01589100	P	69.80	44.60	2.47	2.40	7.40	0.054	94.60	0.32768	9.80E+05	1.52E+06	1.47	0.00119	0.01930	0.01340	0.129
01589300	P	61.40	32.70	32.5	32.60	22.80	0.056	21.30	0.38060	6.83E+06	9.38E+06	1.80	0.00032	0.00305	0.00903	0.554
01589330	P	71.10	49.40	5.52	5.50	7.70	0.047	44.90	0.34929	9.32E+05	1.09E+06	0.92	0.00050	0.00934	0.00900	0.329
01589440	P	47.90	16.60	25.2	25.10	23.80	0.078	32.40	0.36483	3.84E+06	4.57E+06	1.68	0.00035	0.00508	0.01231	0.459
01591000	P	8.90	2.60	34.8	34.90	40.60	0.092	29.80	0.39778	8.40E+06	1.23E+07	2.77	0.00042	0.00383	0.01163	0.482
01591400	P	19.60	5.80	22.9	22.90	23.30	0.080	32.20	0.37147	5.05E+06	7.36E+06	2.56	0.00118	0.00448	0.01120	0.220
01591700	P	25.20	10.10	27	27.30	32.90	0.056	26.50	0.37861	5.76E+06	7.52E+06	1.78	0.00023	0.00406	0.00859	0.438
01593500	P	57.80	28.30	38	38.20	20.70	0.053	18.80	0.40981	6.87E+06	1.14E+07	1.76	0.00013	0.00181	0.00707	0.682
15937100	P	35.00	11.20	48.4	48.00	25.20	0.061	19.20	0.41566	7.05E+06	1.22E+07	2.04	0.00003	0.00210	0.00877	0.697
01594000	P	45.20	19.10	98.4	98.30	24.80	0.059	14.10	0.41919	2.42E+07	3.01E+07	3.14	0.00009	0.00183	0.00837	0.656
01643495	P	0.00	0.00	0.15	0.10	99.70	0.232	1053.50	0.10987	3.97E+05	4.38E+05	0.95	0.14616	0.24892	0.05214	0.000
01643500	P	13.80	4.70	62.8	62.80	43.20	0.103	29.60	0.38186	1.65E+07	2.51E+07	3.90	0.00029	0.00406	0.01119	0.469
01645000	P	40.90	23.90	101	102.00	15.80	0.073	15.40	0.40532	1.48E+07	2.56E+07	3.35	0.00018	0.00252	0.00890	0.611
01645200	P	63.80	40.50	3.7	3.70	8.60	0.055	62.50	0.31184	4.36E+05	5.27E+05	0.79	0.00168	0.01581	0.01135	0.079
01651000	P	62.30	27.50	49.4	49.40	16.70	0.066	20.50	0.37950	1.89E+07	2.13E+07	2.64	0.00027	0.00305	0.00897	0.471

Bibliography

Bonnin, Geoffrey M., Martin, D., Lin, B., Parzybok, T, Yekta, M. and David Riley, (2004). "Precipitation-Frequency Atlas of the United States." NOAA Atlas 14., Vol. 2. U.S. Department of Commerce, Silver Spring, Maryland.

Chow,V.T., (1959). *Open channel Hydraulics*. Mc Graw-Hill, New York.

Dillow, J.J.A., (1997). *Techniques for simulating peak-flow hydrographs in Maryland*: U.S. Geological Survey Water-Resources Investigations Report 97-4279.

Eagleson, P.S.,(1962). "Unit Hydrograph Characteristics for Sewered Areas." J. of Hydraulic Division, ASCE, Vol. 88.HY2.

Eaton, T.D. (1954). "The Derivation and Synthesis of the Unit Hydrograph when Rainfall Records are Inadequate." Inst. Engin. Austral. Jour., Vol. 26:239-243.

Federal Aviation Agency, (1970). "Department of Transportation Advisory Circular on Airport Drainage." Rep. A/C 150-5320-5b, Washington D.C.

Izzard, C.F., (1946). "Hydraulics of runoff from developed surfaces.", Proc. Highway Research Board, Vol. 26: 129-146.

Kirpich, Z.P., (1940). "Time of concentration of small agricultural watersheds." Civil Engineering, Vol. 10(6): 362.

Maryland Department of Planning (MDP). GIS data download. Land use (1990 and 2000). <http://www.mdp.state.md.us/zip_downloads_accept.htm>, (January, 2007).

McCandless, Tamara L. and Richard A. Everett, (2002)." Maryland Stream Survey: Bankfull Discharge and Channel Characteristics of Streams in the Piedmont Physiographic Region." U.S. Fish & Wildlife Service, Chesapeake Bay Field Office, CBFO-S02-01.

McCandless, Tamara L., (2003a). "Maryland Stream Survey: Bankfull Discharge and Channel Characteristics of Streams in the Allegheny Plateau and the Valley and Ridge Physiographic regions." U.S. Fish & Wildlife Service, Chesapeake Bay Field Office CBFO-S03-01.

McCandless, Tamara L., (2003b). "Maryland Stream Survey: Bankfull Discharge and Channel Characteristics of Streams in the Coastal Plain Physiographic region." U.S. Fish & Wildlife Service, Chesapeake Bay Field Office CBFO-S03-02.

McCuen, R.H., S.L. Wong, and W.J. Rawls, (1984). "Estimating Urban Time of Concentration." J. Hydraulic Engineering, ASCE, Vol. 110 (7):887-904.

McCuen, R.H., (2005). *Hydrologic Analysis and Design, 2nd Edition*, Prentice Hall, Inc., New Jersey.

McCuen, R.H., (2005). Numerical Optimization FORTRAN program (NUMOPT).

Morgali, J.R. and R.K. Linsley, (1965). Computer analysis of overland flow, Hydraulic Division. ASCE, Vol. 91 (HY3): 81-100.

National Operational Hydrologic Remote Sensing Center (NOHRS, 2005). Unit Hydrograph (UHG) Technical Manual. <http://www.nohrsc.nws.gov/technology/gis/uhg_manual.html>, (January, 2007).

Pavlovic, S.B and G.E.Moglen, (2007). "Discretization Issues in Travel Time Calculation." J. Hydrologic Engineering, ASCE. (in press).

Singh, V.P., (1989). *Hydrologic Systems: Watershed Modeling*. Vol. 2. Prentice-Hall, Inc., Upper Saddle River, N.J.

Soil Conservation Service (SCS, 1972). "Travel time, time of concentration and lag." Nation Engineering Handbook (NEH): Chapter 15.

< http://www.wcc.nrcs.usda.gov/hydro/hydro-techref-neh-630.html>, (December, 2005).

Soil Conservation Service (SCS, 1986). *Urban Hydrology for Small Watersheds*, Tech. Release No. 20, Washington D.C.

Thomas, W. O. Jr., Monde, M. C. and S. R. Davis., (2000). "Estimation of Time of Concentration for Maryland Streams." Transportation Research Record, Vol. 1720:95-99.

U.S. Army Corps of Engineers, (2001). HEC-HMS Hydrologic Modeling System. User's Manual. Version 2.2.1.

U.S. Army Corps of Engineers, (2004). HEC-RAS River Analysis System. Hydraulic Reference Manual. Version 3.1.1. US Geological Survey (USGS), (2006). National Hydrograph Dataset (NHD).

U.S. Geologic Survey, Geographic Data Download. Geographic Information Retrieval and Analysis System (GIRAS) land use data. <http://edc.usgs.gov/geodata/>, (August, 2006).

U.S. Environmental Protection Agency, (2005). "EPA MRLC National Land Cover Data (NLCD)." < http://www.epa.gov/mrlc/nlcd.html>, (January, 2007).